Research Project

GlacierRocks

Glacier-Headwall Interaction and its Influence on Rockfall Activity

Final Report (2017-2020)

Imprint

Editor: GEORESEARCH Forschungsgesellschaft mbH, Hölzlstraße 5, 5071 Wals b. Salzburg

Authors: Ingo Hartmeyer, Kay Helfricht, Kerry Leith, Markus Keuschnig, Andreas Ewald, Robert Delleske, Jan-Christoph Otto, Michael Krautblatter

Project Partners: GEORESESEARCH, IGF – Institut für Interdisziplinäre Gebirgsforschung, ETH Zürich, Universität Salzburg, TU München

Funding: ÖAW – Austrian Academy of Sciences

Cover Photo: Randkluft, Kitzsteinhorn north-face (Robert Delleske, 13.09.2019)

ISBN-Online: 978-3-7001-8361-7

DOI: 10.1553/ESS-GlacierRocks

Abstract

The three-year (2017-2020) research project GlacierRocks combined the geomorphological and glaciological expertise of several international project partners to study poorly understood stability-relevant processes and rockfall activity at the glacier-headwall-interface. The project comprised challenging high-alpine fieldwork and laborious data analyses that were translated into a substantial publication output, contributions to diploma and PhD theses, and targeted media activities leading to prominent newspaper articles and TV documentaries.

During an extensive field campaign an unprecedented monitoring of bedrock and ice temperatures inside a randkluft (gap between glacier and headwall) was established at the Kitzsteinhorn, Hohe Tauern Range, Austria. The installed monitoring represents the first of its kind worldwide and allowed unique insights into the thermal state of the glacier-headwall-interface and climate warming-related changes. The investigated randkluft is located at 2 900 m a.s.l. in a northeast-facing headwall. Bedrock and ice temperature measurements were carried in depths of up to 15 m below glacier surface level. Fieldwork inside the narrow confines of the randkluft was restricted to a seasonal time window of about six weeks and proved to be technically challenging.

Mean annual bedrock temperatures measured inside the randkluft (-0.3 to -0.5 °C) were warmer than in the rockwall above the glacier (-0.8 to -2.7 °C) suggesting rockwall cooling in freshly deglaciated (north-facing) headwall sections. Thermal variability inside and above the randkluft differed considerably. In the open rockwall above the glacier seasonal amplitudes between 20 °C and 30 °C were observed. Inside the randkluft at 15 m depth below the glacier surface near-isothermal behavior with annual variations of less than 1 °C were recorded. Despite being warmer than the open rockwall above, bedrock temperatures inside the randkluft remained at or slightly below 0 °C for the entire year. Glacial downwasting is therefore expected to induce the formation of an active layer in the summer season that runs in parallel to the proposed average cooling of the exhumed rock mass. Active layer formation, which may occur for the first time since mid-Holocene times, is expected to induce thermal stress, reduce rock stability through warming/melting of interstitial ice, and eventually increase rockfall susceptibility in freshly deglaciated terrain.

Mean annual glacier ice temperatures inside the randkluft (measured 7 and 15 m below the glacier surface) ranged around -0.3 °C and thus appear to be slightly warmer than mean bedrock temperature. The randkluft may therefore govern the interaction between a warmer ice mass and a cooler rock mass. In late spring the entire investigated ice mass (15 m depth) rapidly warms and reaches near-isothermal state with temperatures just below 0 °C within just two weeks. This sharp increase of the glacier ice temperature is most likely caused by extensive meltwater refreezing at the snow-ice-interface or meltwater percolating into the ice volume, which is expected to release high amounts of energy by latent heat. No such rapid warming was observed in the headwall which is adjusting to increasing seasonal air temperature at a much slower pace. The observed intense late-spring warming of the glacier ice is countered by slow ice cooling in winter that is impeded by a thick insulating snow cover. This contrast creates a vertical thermal offset inside the glacier and clearly demonstrates how glaciers act as thermal filters that efficiently promote the propagation of subzero temperatures immediately below the melting point.

Parallel to the in-situ monitoring inside the randkluft a unique rockfall inventory was compiled for the rockwalls of two neighboring cirques in the summit region of the Kitzsteinhorn. During the monitoring 632 rockfalls were registered ranging from 0.003 to 879.4 m³, mainly originating from pre-existing structural rock weaknesses. 60 % of the rockfall volume detached from less than ten vertical meters above the glacier surface, 75 % within the first twenty meters above the glacier, indicating enhanced rockfall activity over tens of years following deglaciation. Increased mass wasting activity in recently deglaciated areas, such as discovered in the present study, is typical of paraglacial environments, where slope systems gravitationally adjust to new, non-glacial boundary conditions. Previous studies

on the paraglacial adjustment of bedrock slopes mostly focused on high-magnitude events such as rock avalanches and rockslides, which commonly respond to deglaciation on centennial to millennial time scales. The lower end of the paraglacial magnitude-frequency spectrum is currently poorly characterized. The present study bridges this gap and for the first time provides field evidence of an immediate, low-magnitude paraglacial response in a currently deglaciating rock slope system.
Debuttressing seems to play a minor effect only. Rather, preconditioning is assumed to start inside the randkluft where sustained freezing and ample supply of liquid water likely cause enhanced physical weathering and high plucking stresses. Following deglaciation, pronounced thermomechanical strain is induced and an active layer penetrates into the formerly perennially frozen bedrock. These factors likely cause the observed paraglacial rockfall increase close to the glacier surface. The conducted study presents the most extensive dataset of high-alpine rockfall to date and the first systematic documentation of a cirque-wide erosion response of glaciated rockwalls to recent climate warming.

Executive Summary

The following executive summary of the ÖAW-funded research project *GlacierRocks* is directed at policymakers, practitioners and a wider audience interested in the consequences of climate change in high-alpine regions. It complements the above scientific abstract and provides a plain language synopsis of a long-term rockwall monitoring which identified **increased rockfall activity in terrain exposed by recent glacier thinning**.

In the last 150 years mean annual air temperatures in Austria have risen by 2 °C, which is about twice as high as the average global warming rate. Over the same time span glaciers in Austria lost around half of their area and volume as glacier retreat has become one of the most visible consequences of climate warming. The rate of glacier retreat has increased since the 1980s, **with much of the volume loss being reflected by the lowering of the ice surfaces even in the uppermost parts of alpine glaciers.**

In the present study we monitored rockwalls in the summit region of the Kitzsteinhorn (3203 m a.s.l.) for six years (2011-17) with remote sensing (terrestrial laserscanning) to identify rockfall source areas. All monitored rockwalls are situated directly adjacent to the Schmiedingerkees glacier, which currently lowers its surface by about 0.7 m per year in the uppermost parts. During the monitoring we identified over 600 rockfall source areas, which makes the compiled dataset the most extensive record on high-alpine rockfall to date worldwide. We observed **drastically increased rockfall activity following ice retreat** as 60 % of the rockfall volume detached from less than ten meters above the glacier surface – i.e. from areas that were **freshly exposed by glacier retreat** in recent years and decades.

To investigate the causes behind the rockfall increase following glacier retreat, we conducted unprecedented temperature measurements in rockwall sections that are still covered by glacier ice. The initiated multi-year monitoring showed little seasonal variation and temperatures just below 0 °C inside the randkluft (void between glacier and rockwall). As the glacier is wasting down an unfrozen layer is forming, water is infiltrating joints and fractures, and winter/summer temperatures penetrate into the exposed rockwall, all of which exert a **significant destabilizing influence on rockwall sections exposed by current glacier retreat**.

The monitoring results are important for rockfall hazard assessments as they indicate that in rockwalls affected by glacier retreat historical rockfall patterns may no longer be used as indicators for future events. Recurrence intervals of different events likely change with time since deglaciation, which is helpful information for **infrastructure managers in high-alpine regions including operators of cable cars, storage lakes, alpine routes and mountain huts**. Increased rockfall activity is particularly critical in glacial environments due the presence of glacially oversteepened rockwalls and low-friction glacier surfaces, which both promote long rockfall runout distances. Many high-alpine infrastructure operators may therefore have to adapt risk-reduction measures in the near future.

Models suggest a temperature increase of 1.5 °C over the next 30 years in Austria, which will further accelerate the dramatic retreat of glaciers currently observed. By the end of the century glaciers in Austria are expected to decrease to less than 20 % of today's area. Glacier retreat will therefore continue to alter the face of the Alps and elevated rockfall from freshly exposed rockwalls – quantified systematically in this project for the first time – **will be of growing relevance for stakeholders, practitioners and scientists.**

Content

Report Structure

This report summarizes the main activities and results of the three-year research project *GlacierRocks – Glacier-Headwall Interaction and its Influence on Rockfall Activity*. The report is structured as follows:

Chapter 1 gives a brief introduction addressing the significance of recent glacier retreat in the Alps, destabilization/rockfall in deglaciating rockwalls, and the lack of knowledge on thermal, mechanical and hydrological processes at the glacier-headwall-interface.

Chapter 2 introduces the project's study area and gives an overview of the Open-Air-Lab Kitzsteinhorn (OPAL), which provided valuable complementary data and will serve as a platform for the continuation of the monitoring activities after the conclusion of *GlacierRocks*.

Chapter 3 details the findings of a unique bedrock and ice temperature monitoring inside and above a randkluft, which contribute to an improved understanding of the thermal state and dynamics at the headwall-glacier-interface.

Chapter 4 summarizes an unprecedented rockfall inventory compiled at the Kitzsteinhorn, which revealed significantly increased rockfall activity in recently deglaciated rockwall sections and points to antecedent rockfall initiation inside the randkluft.

Chapter 5 outlines the results of a regional-scale GIS study which identified deglaciating headwalls based on morphometric parameters in the Hohe Tauern Range.

Chapter 6 describes the efforts made to establish a cutting-edge microclimatic and acoustic emission monitoring inside a challenging randkluft environment.

Chapter 7 provides a short outlook on the continuation of the established monitoring and on the growing relevance of the investigated subject in a warming climate.

Chapter 8 lists the project's comprehensive publication, spearheaded by two manuscripts recently published in *Earth Surface Dynamics* (Hartmeyer et al. 2020a, Hartmeyer et al. 2020b) focussing on the impacts of glacier retreat on rockfall activity.

1. Introduction

Since 1880 mean annual air temperatures in Austria have risen by 2 °C (APCC 2014). This increase is more than twice the average global warming of 0.85 °C over the same time span. Glacier retreat has evolved into one of the most visible consequences of climate warming in the 20th and 21st century in the European Alps (Lambrecht & Kuhn 2007, Fischer 2009). The glaciers in Austria lost 56% of their total area since the end of the Little Ice Age around 1850 (Fischer et al. 2015). In the same time an estimated 50 % of the original glacier volume in the European Alps has disappeared (Haeberli & Hoelzle 1995). The rate of retreat has increased since the 1980s, with much of the volume loss being reflected by the lowering of the ice surfaces (Haeberli et al. 2007). Models suggest that a mean summer temperature rise by 3 °C will lead to a decrease to less than 20 % of today's glacier area in Austria within this century (Zemp et al. 2006).

While geomorphological and glaciological research has often focused on the effects that retreating glaciers have on their forefields, interactions between diminishing accumulation zones and oversteepened glacial headwalls have received comparatively little attention. In proglacial areas melting glacier tongues expose mostly smooth, gently to moderately inclined terrain. Within the glacial accumulation areas, however, glacier retreat exposes oversteepened headwall sections that are highly susceptible to rockfall. Lowering of the glacier surface leaves adjacent headwalls without glacial abutment and exposes bedrock surfaces to atmospheric influences, potentially for the first time in many millennia. Understanding the spatio-temporal dynamics of these interactions is of high importance to identify operating processes and quantify their impact. It will also allow developing predictive models to help coping with the impacts of the present climate warming in high mountain environments.

Within the context of a rapidly warming climate, not only in the European Alps but also in mountain regions worldwide, steep, currently glacier-covered headwall sections that will soon be exposed through glacial thinning are highly of direct relevance. Headwalls are primary source areas of debris input into the glacier system and thus one prerequisite for glacial erosion. However, despite their importance for the understanding of erosional processes and high-alpine rockfall, little is known about the thermal, mechanical and hydrological processes that operate at the glacier-headwall-interface. Mass and energy exchange at this interface is governed by seasonally air- or snow-filled voids (randkluft) of variable width and depth. The evolution of a randkluft system is affected by changes in the entire glacial system not just the accumulation zone. Due to glacier thinning large valley glaciers showed a strong reduction of flow velocities in the last decades (Span et al. 1997, Stocker-Waldhuber et al. 2019). The reduced mass transport has some stabilizing effect on glacier surface elevations in present accumulation zones. However, extremely warm summers of the last years caused high sliding velocities because of increased meltwater availability at the glacier bed, as evidenced by the formation of large crevasses and wide randklufts. Caused by temperature increase, the base of small cold-based glaciers underwent a change to melting conditions and initiated glacier movement and randkluft formation (Benn & Evans 2010). So far direct observations of randkluft environments are very rare due to highly restricted accessibility and extremely harsh measurement conditions. The few existing investigations rely on air temperature measurements in the upper reaches of randkluft systems (Gardner 1987). In-situ measurements of rock (and glacier ice) temperature, rock moisture and frost cracking that are essential for understanding the physical processes do not exist. Hypotheses on the efficacy of various processes that precondition headwalls for rockfall triggering (e.g. frost weathering) have therefore remained untested.

Better understanding of glacier-headwall-interactions is essential as high rockfall activity in recently exposed headwall sections represents a considerable risk factor (Hock et al. 2019). With continuing warming, the significance of randkluft-related risks is expected to grow throughout the near future. The combination of oversteepened headwalls and steeply inclined glacier surfaces with low

damping/friction conditions results in long runout distances of detached blocks that represent potentially serious threats to man and high-alpine infrastructure (Deline et al. 2015). On regional or mountain range scales, hazard severity and extent of affected areas are largely unknown, significantly impeding adaptation and mitigation measures. From an alpinistic/touristic perspective the observed, warming-related widening of randklufts (and bergschrunds) represents a growing concern that has not only negatively affected the accessibility of numerous popular alpine routes but also represents a serious and increasing hazard for alpinists. These problems clearly underscore the importance of a better understanding of the highly dynamic interactions between shrinking glaciers and their adjacent headwalls.

In line with these research gaps the project *GlacierRocks* has established the first long-term monitoring site for rock and glacier ice temperatures inside a randkluft system to investigate the thermal state and dynamics at the glacier-headwall-interface (Chapter 3). Furthermore an extensive rockfall inventory was compiled for deglaciating rockwalls, which represents the largest of its kind worldwide and provides unique insights into rockfall activity in headwalls exposed by recent glacier retreat (Chapter 4). On a regional scale, deglaciating headwalls in the Hohe Tauern Range were identified based on morphometric parameters in a comprehensive GIS analysis (Chapter 5). Finally, the established randkluft monitoring will be integrated into the research infrastructure of the Open-Air-Lab Kitzsteinhorn to allow the long-term continuation of the initiated measurements.

2. Study Area

Since 2010 the summit region of the Kitzsteinhorn is home to an interdisciplinary Open-Air-Lab (Figure 1) focusing on the interaction between rockfall and mountain permafrost (Keuschnig et al. 2015). The systemic long-term monitoring at the Kitzsteinhorn intends to reduce research gaps between lab experiments and significantly more complex real-world conditions. The existing research infrastructure includes several deep and shallow boreholes (Hartmeyer et al. 2012), a permanently installed electrical resistivity tomography profile (Keuschnig et al. 2016), rock anchor load loggers (Plaesken et al. 2017), extensometers in fractures (Ewald et al. 2019) and several fully automated weather stations. The existing research base served as valuable complementary support during the entire project and created valuable synergy effects.

Several closely collaborating projects are based at the Kitzsteinhorn (SeisRockHT, MOREXPERT I + II), contributing to the national and international visibility of the site (AlpHaz 2020, GTN-P 2020). The tourism infrastructure existing within the study area (cable car, ski lifts) provided easy access and convenient transportation, an essential prerequisite during the establishment of an extensive long-term monitoring program.

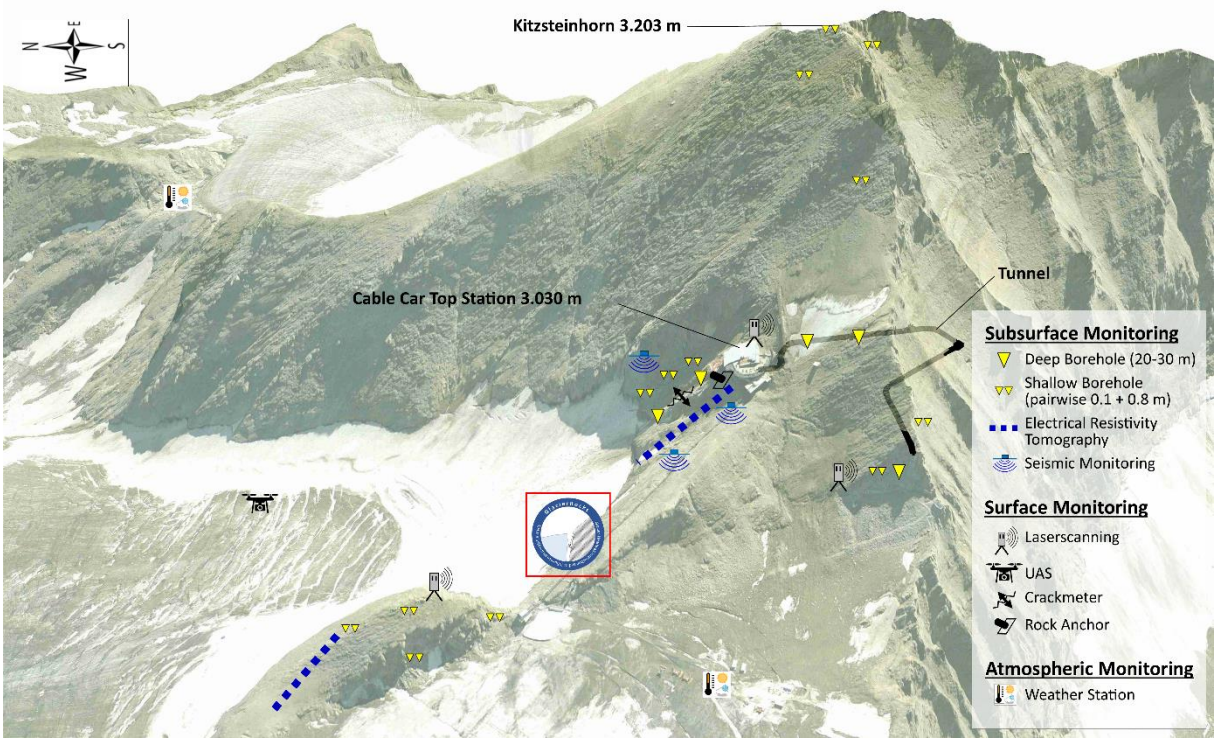

Figure 1: Schematic illustration of the Kitzsteinhorn Open Air Lab (OPAL) and its monitoring installations. The GlacierRocks project logo (surrounded by red square) indicates position of the established randkluft monitoring (Chapter 3).

3. Thermal State and Dynamics of the Headwall-Glacier-Interface in a Warming Climate

To investigate the thermal state of deglaciating rockwalls a northeast-facing headwall section at the Kitzsteinhorn was selected for temperature monitoring (Figure 2). Randkluft development at the chosen site showed significant interannual variation. Access to the randkluft was usually possible from mid-August to early October, which left a narrow annual time window of about six weeks for fieldwork. In 2017 heavy snowfalls covered the randkluft by the first week of September while in 2018 fieldwork inside the randkluft was possible until late October.

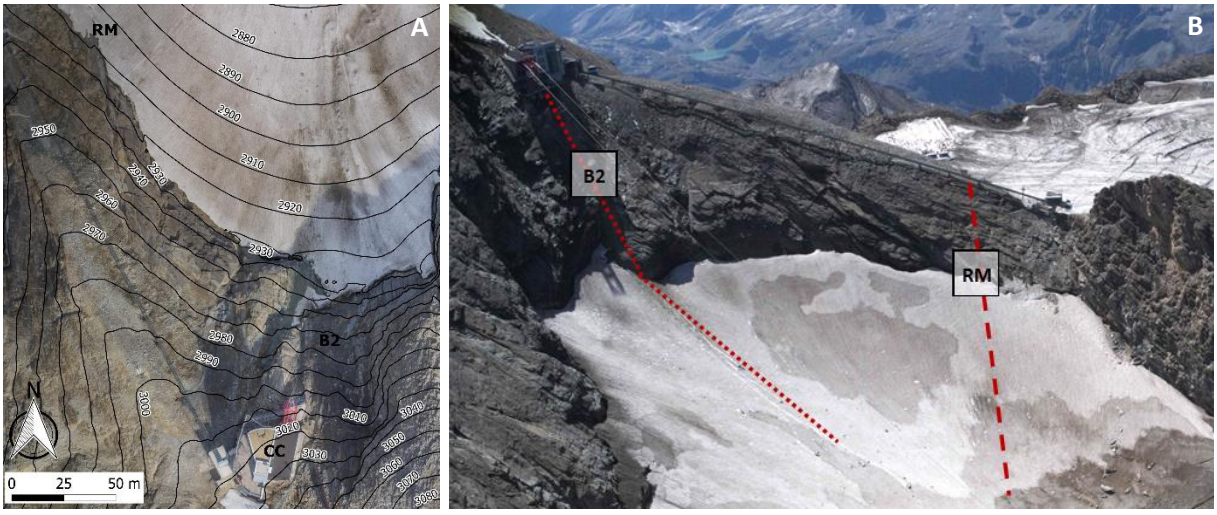

*Figure 2: (**A**) Orthophoto of study site; (**B**) Oblique view of the investigated glacier-headwall system. Dotted line: 2D profile line used for Figure 5A; Dashed line: 2D profile line used for Figure 5B (Photo: R. Delleske, 24.08.2017). Abbreviations: (RM) Randkluft Monitoring; (B2) Borehole (30 m); (CC) Cable car top station.*

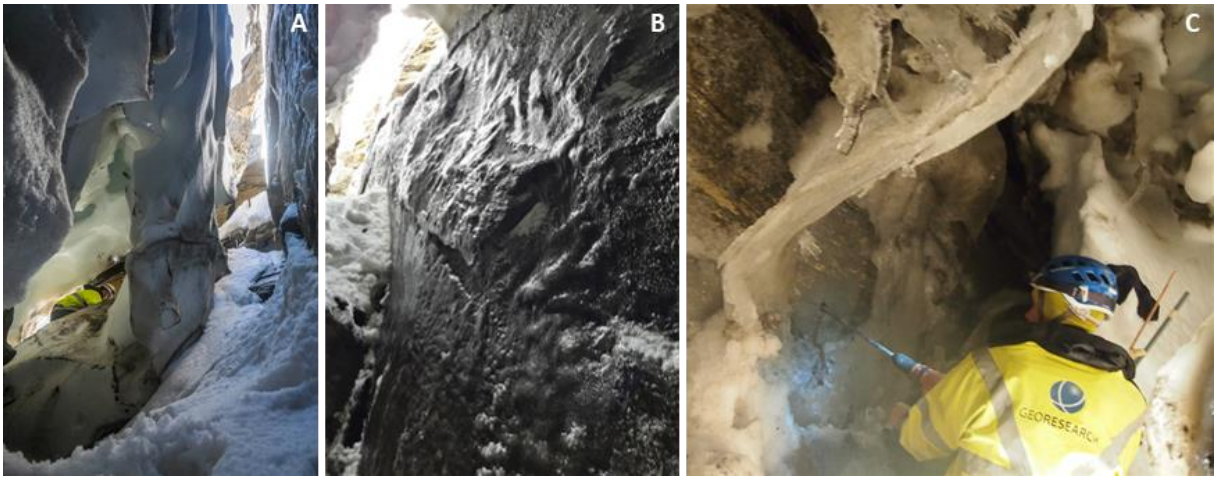

*Figure 3: (**A**) Ice bridge between glacier (left) and rockwall (right); (**B**) Vertical headwall section immediately above MS Randkluft Deep covered with thin ice coating ('verglas'); (**C**) Drilling works 15 m below the glacier surface.*

The width of the randkluft opening ranged between half a meter and one meter, randkluft widths near the monitored transect showed great variation and ranged between complete closure and broad gaps spanning several meters. Significant variations were also observed *inside* the randkluft. While large structures (e.g. ice bridges, wedged rockfall deposits) mostly remained unchanged over the years (Figure 3A), remarkable changes of the randkluft 'topography' were caused by inter-annually varying snow infill, ice formation and ice melt. The observed significant changes between the years are unlikely of glaciological origin (e.g. submergence), but are much rather caused by infiltrating melt- and rainwater causing rapid snow- and ice melt and/or new ice formation. The input of liquid water into

the randkluft system may therefore represent one of the key agents of randkluft formation and development, and may exert a significant influence on the efficacy of frost weathering processes and glacial plucking stresses.
The constantly changing topography of the monitored randkluft posed a considerable challenge for the installation works. Rappelling routes and climbing bolts had to be renewed almost every year. The monitored randkluft transect was relatively well shielded from rockfalls. To further minimize rockfall risk, the rockwall section above the randkluft was cleared from loose fragments and blocks. The biggest threat during installation and maintenance works was posed by unstable ice inside the randkluft. Due to the confined space of the randkluft, navigation was complicated particularly during equipment transport. Below a depth of approximately 12 m, complete darkness further impeded orientation. The deepest point reached was approximately 17 m below the glacier surface.

3.1. Temperature Measurement

For temperature measurement, wireless miniature data loggers were used (Geoprecision M-Log5W-Rock) (Figure 4). The loggers contain PT1000 thermistors, which measure temperature with an accuracy of ± 0.1 °C and a resolution of 0.01 °C. The loggers are protected by a robust stainless steel housing (IP 69) and have a high storage capacity of up to 400.000 measurements. Due to their small dimensions and their low energy consumption, the loggers are well-suited for long-term operation under harsh, high-alpine conditions. Energy is supplied by removable AA lithium batteries, which ensure uninterrupted runtimes of several years. Data readout is conducted via a wireless interface (433/915 MHz) and was successfully performed even when the loggers were covered by several meters of snow.

Figure 4: Miniature temperature logger (Geoprecision M-Log5W-Rock) installed 7 m below the glacier surface ('Randkluft Deep'). The wooden beam protects the logger from falling ice and rocks.

3.2. Monitoring Setup

The randkluft monitoring was established in a northeast-facing headwall section approximately 200 m from the cable car top station. Five different measurement sites (MS) were equipped with temperature sensors: (i) *MS Rockwall* (2915 m a.s.l.) located 9 m above the randkluft lip, (ii) *MS Randkluft Lip* (2906 m a.s.l.) located at glacier surface level, (iii) *MS Randkluft Deep* (2899 m a.s.l.) located 7 m below the glacier surface in a vertical rockwall section, (iv) *MS Randkluft Dark* (2891 m a.s.l.) located 15 m below the glacier surface, and (v) *MS Glacier* (2903 m a.s.l.) located 6 m from the randkluft lip at the glacier surface (Figure 5).

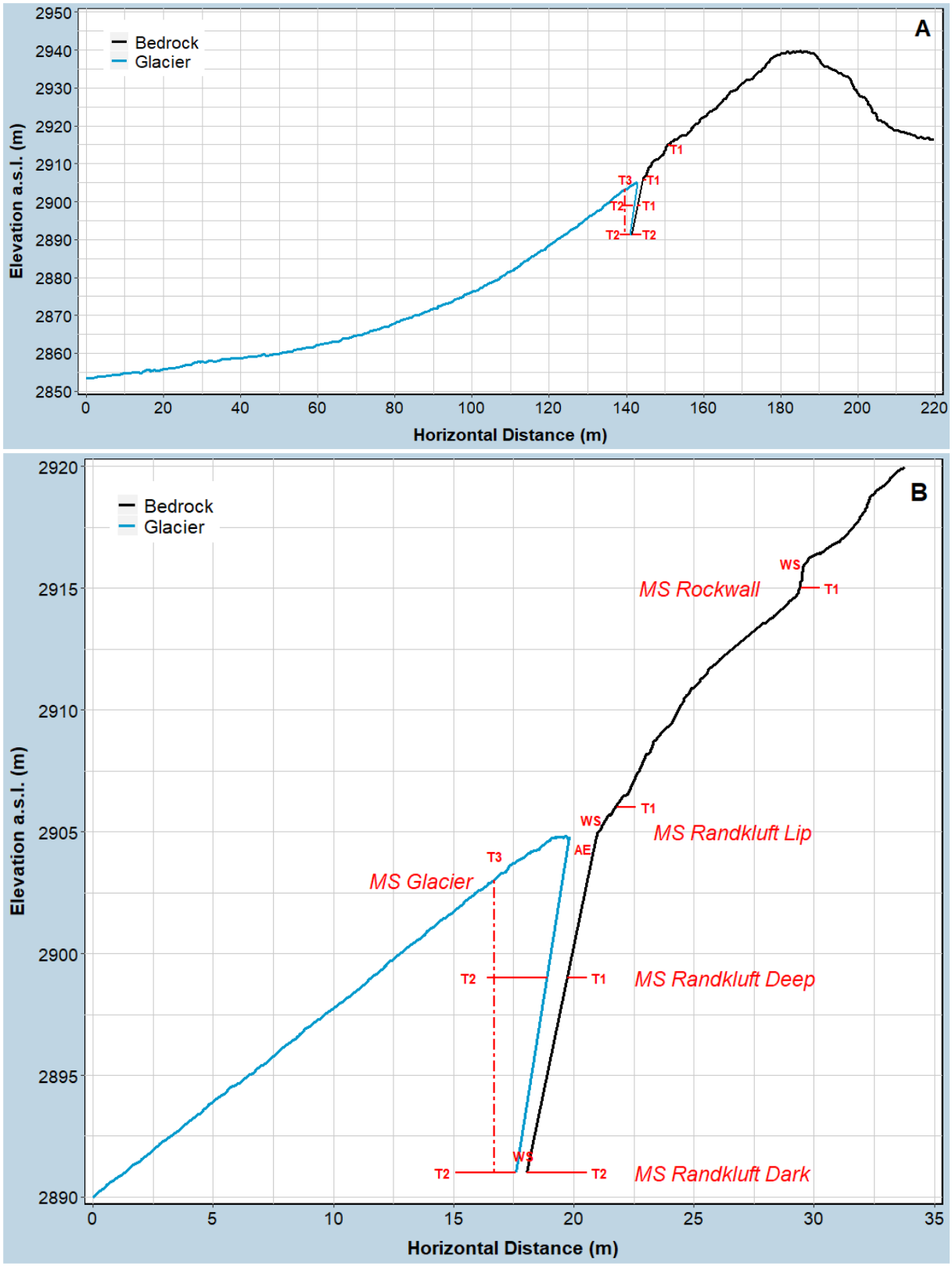

*Figure 5: 2D cross section of the investigated glacier-randkluft-headwall system – (**A**) Slope scale (top), (**B**) Randkluft scale (bottom). Terrain surface data is derived from TLS and UAV surveys carried out in 2019. Randkluft depths were recorded with measuring tapes. Rockwall gradients inside the randkluft were estimated. (T1) temperature measurement at 0.1 and 0.8 m borehole depth; (T2) temperature measurement at 0.1, 0.8 and 2.5 m borehole depth; (T3) temperature measurement at 1, 2, 4, 6, 8, 10, 12 m depth; (MS) Measurement site; (WS) Miniature weather station; (AE) Acoustic emission monitoring.*

MS Rockwall is located in a north-east exposed section of the headwall which follows an average gradient around 45° consistent with the cleavage of the local micaschists. Rock temperature at MS Rockwall is measured at 0.1 and 0.8 m borehole depth. MS Randkluft Lip is located at glacier surface

level, several meters below a significant gradient break (schrundline), typical of (formerly) glaciated headwalls (Gilbert 1904, Sanders et al. 2012). Rock temperature at MS Randkluft Lip is measured at 0.1 and 0.8 m borehole depth. MS Randkluft Deep is situated in a steep section, vertically below MS Randkluft Lip. Rock temperature is measured at 0.1 and 0.8 m borehole depth, glacier ice temperature is measured at 0.1, 0.8 and 2.5 m depth. MS Randkluft Dark is located 15 m below the glacier surface and around 15 m west of MS Randkluft Deep. Rock and ice temperature are both measured at 0.1, 0.8 and 2.5 m borehole depth at Randkluft Dark. MS Glacier is represented by a 12 m deep vertical borehole drilled into the glacier. The borehole was equipped with a temperature string consisting of seven sensors mounted on a wooden stick (sensor depths: 1, 2, 4, 6, 8, 10, 12 m).
Bedrock drilling was performed with a battery driven drill hammer (Hilti TE 6) and a drill diameter of 8 mm for all measurement sites except MS Randkluft Dark. At MS Randkluft Dark a corded rotary hammer (Hilti TE 70) with a drill diameter of 32 mm was used to reach a borehole depth of 2.5 m (Figure 3C). Ice drilling works were carried out with a steam-driven ice drill (Heucke ice drill). All boreholes (bedrock and ice) were drilled perpendicular to the local terrain surface (i.e. horizontal drilling direction for all sites except MS Glacier).
Temperature data from a nearby 30 m deep borehole (MS B2) was used to complement and validate the analysis of the temperature data acquired inside the randkluft. MS B2, which is part of the research infrastructure of the Open-Air-Lab Kitzsteinhorn, is located around 50 m from the cable car top station at 2985 m a.s.l. and is currently situated approximately 40 vertical meters above the current glacier surface.

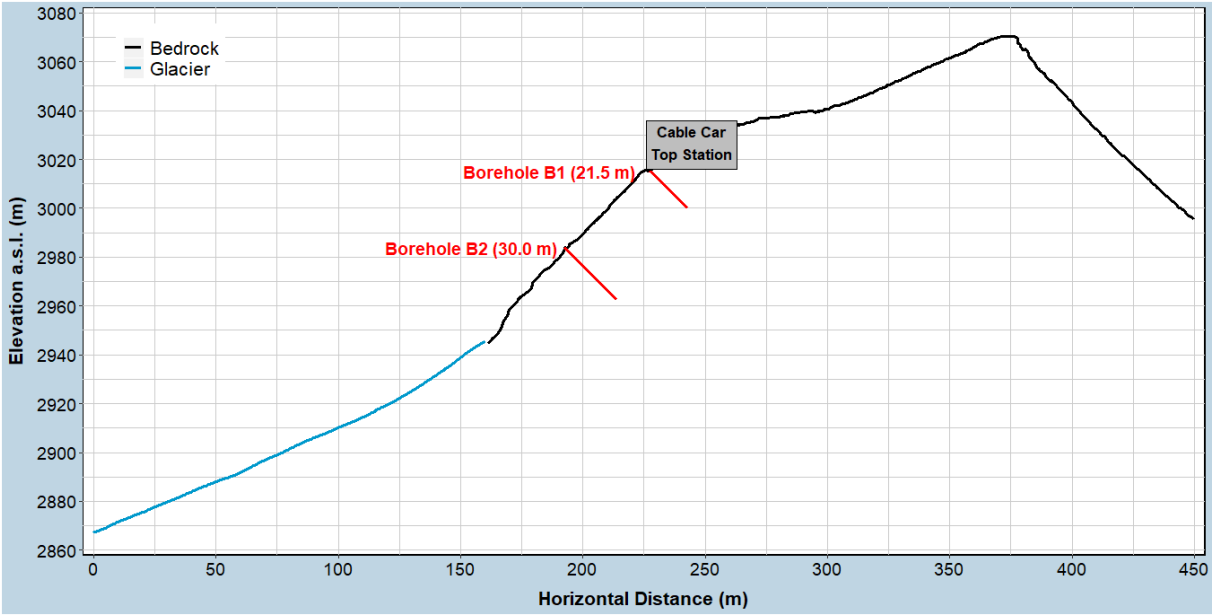

Figure 6: 2D slope profile across cable car top station (3015 m a.s.l.) and Borehole B2 (2985 m a.s.l.). The deepest sensor of B2 (30 m depth) is situated around 18 vertical meters above the current glacier surface.

3.3. Results & Interpretation

3.3.1. Bedrock Temperature

Thermal conditions inside and above the randkluft differed significantly during the four-year observation period (Oct 2015 to Sep 2019) (Figure 7). In the rockwall above the randkluft (MS Rockwall, MS B2) near-surface measurements at 0.1 m depth showed large annual amplitudes of around 20 °C at MS Rockwall and 30 °C at MS B2. Winter temperature at MS B2 (0.1 m borehole depth) dropped to minimum values of -21.9 °C indicating the absence of a thick insulating snow cover. MS Rockwall was warmer due to significant snow accumulation during the winter season with minimum temperatures

around -8 °C. During the summer season maximum temperatures at the more sun-exposed northeast-facing MS Rockwall were higher (16 °C) than at the north-facing MS B2 (13 °C), which in addition receives more shade by the Kitzsteinhorn summit pyramid.

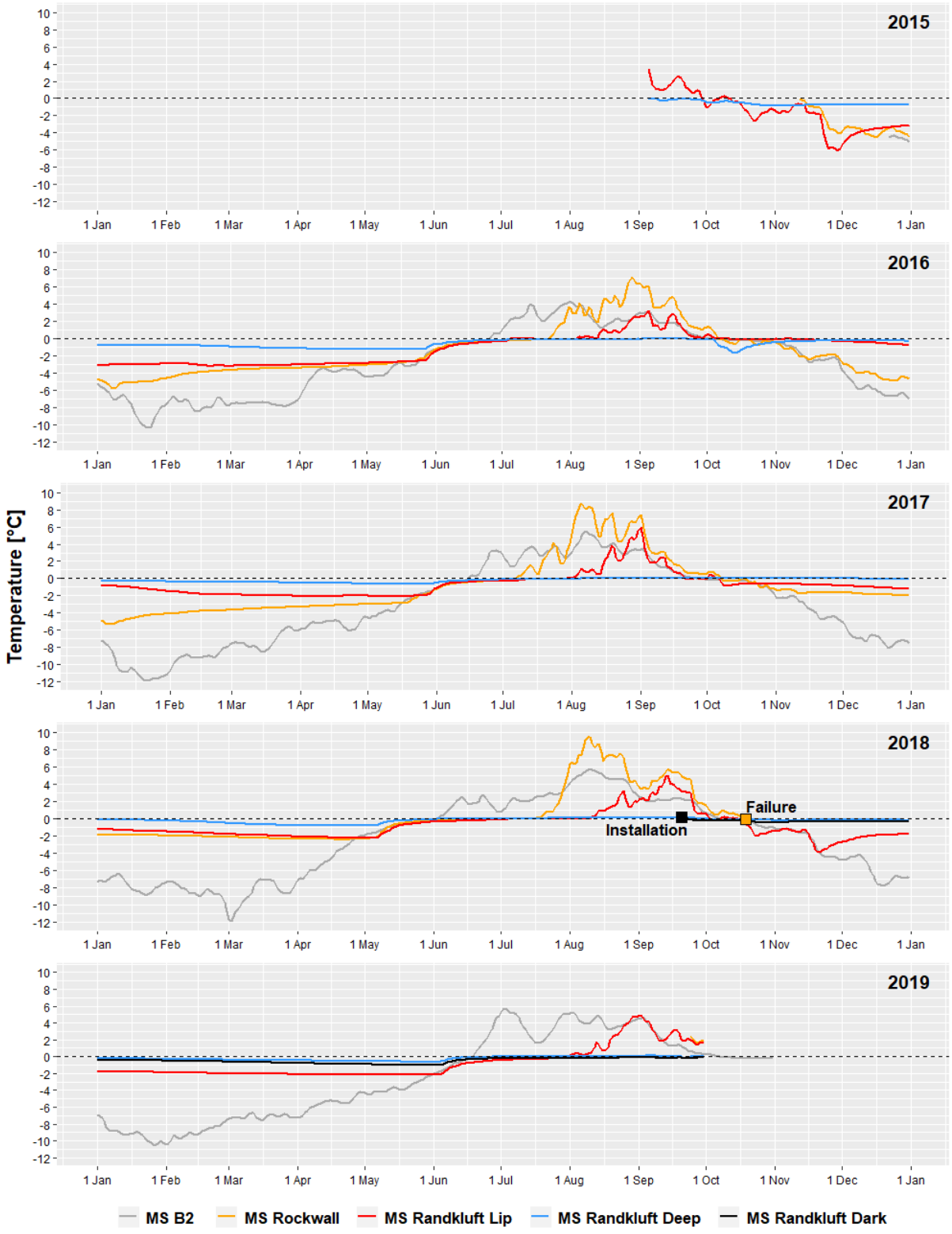

Figure 7: Near-surface bedrock temperature data for the period 2015-2019 taken at 0.8 m borehole depth (temperature at MS B2 was measured at 1.0 m borehole depth).

Bedrock temperature inside the randkluft (MS Randkluft Deep, MS Randkluft Dark) showed little variability. The annual temperature amplitude was attenuated significantly with increasing randkluft depth. At MS Randkluft Lip an annual amplitude of 10-15 °C was recorded, at MS Randkluft Deep temperature varied by 4 °C annually and at MS Randkluft Dark near-isothermal behavior with annual variations of less than 1 °C were measured (all values refer to 0.1 m borehole depth).

Timing and magnitude of autumn snowfall plays a critical role for the annual temperature regime of the randkluft. In autumn 2015, the randkluft was not completely snow-covered until early December allowing sustained penetration of cold air into the randkluft. The resulting cooling led to a prolonged depression of the bedrock temperature at MS Randkluft Deep that was evident until summer warming in June 2016 brought temperatures back to 0 °C. During each winter season (December until May/June) a slight but steady temperature decline was recorded at MS Randkluft Deep, which is abruptly terminated in late May/June by a rapid temperature increase. The cause of this abrupt temperature increase is unknown but is most likely related to infiltrating meltwater, which refreezes inside the randkluft and releases considerable amounts of latent heat in the process (Chapter 3.3.2). During the summer season, bedrock temperature at MS Randkluft Deep stagnates at almost exactly 0 °C indicating intensive latent heat absorption (zero-curtain effect). The summer regime is then succeeded either by a rapid temperature decrease caused by cold air descending into the randkluft (randkluft open) or by a steady slow decline (randkluft closed due to snowfall).

Mean temperature measured inside the randkluft was warmer than in the rockwall above. At MS Randkluft Dark mean temperature (1 Oct 2018 – 30 Sep 2019) equaled -0.45 °C, the four-year average (2015-19) at MS Randkluft Deep was -0.34 °C. At MS Rockwall (9 m above the glacier surface) a four-year average of -0.83 °C was recorded, while at MS B2 (40 m above the glacier surface) mean temperatures of -2.69 °C (1 m borehole depth) were registered. These findings clearly indicate colder bedrock temperatures in the rockwalls above the glacier than in the ice-covered rockwall sections below the glacier surface (randkluft). However, despite being warmer on average, bedrock temperatures inside the randkluft (MS Randkluft Dark) remain below 0 °C the entire year and active layer formation is completely suppressed. Deglaciation related to recent climate warming may therefore introduce an interesting paradox: (i) exhumed rockwall sections are likely to show a cooling trend – at least in north-facing locations – leading to permafrost aggradation, (ii) at the same time warm summer temperatures will lead to near-surface permafrost thaw (active layer formation) in areas that likely have been frozen since the mid-Holocene (APCC 2014).

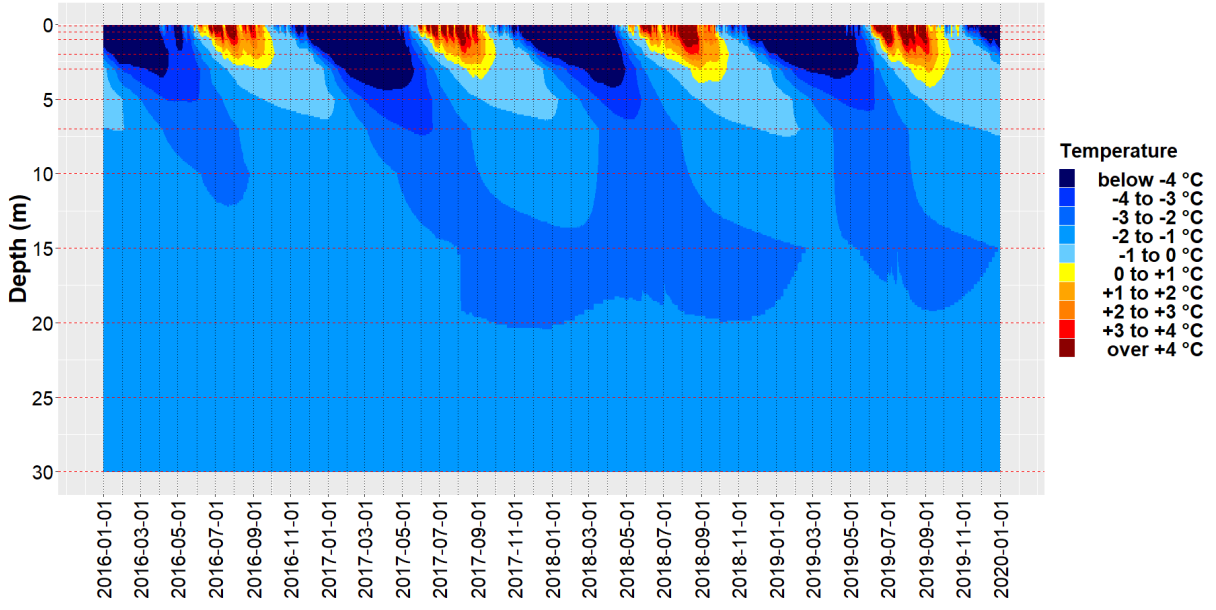

Figure 8: Four-year (2016-19) temperature record from 30 m deep borehole MS B2. Maximum active layer thickness increased from 3 m in August 2016 to 4 m in August 2019.

Borehole data from MS B2 supports this hypothesis. Inside the 30 m deep borehole, temperatures steadily increased with borehole depth, the warmest mean temperatures were recorded at the bottom of the borehole (Figure 8). At 15 m depth mean temperature equaled -2.07 °C, at 30 m depth a mean temperature of -1.80 °C was registered. This significant depth-related warming trend could signify (i) recent surface cooling that is not yet evident at large depths (e.g. related to the recent degradation of local ice faces) (Guglielmin et al. 2018) and/or (ii) an insulation/warming effect by the local cirque glacier (Schmiedingerkees) causing a bedrock temperature increase towards the glacier surface, which is in good agreement with the near-surface temperature data acquired inside and above the randkluft.

3.3.2. Ice Temperature

Mean ice temperatures measured inside the randkluft (MS Randkluft Deep, MS Randkluft Dark) ranged around -0.3 °C and thus showed great similarity with bedrock temperatures. At both sites, mean ice temperature increased with borehole depth – at 2.5 m depth temperatures were about 0.1-0.2 °C warmer than at 0.1 m depth. This pattern contrasts with bedrock temperature measurements carried out at MS Randkluft Dark, which showed a slight temperature *decrease* with borehole depth (no such comparisons were possible for MS Randkluft Deep due to a sensor failure at 0.1 m and the absence of a bedrock temperature sensor at 2.5 m). Longer temperature records are needed to validate the discovered horizontal thermal gradient across the ice/rock-interface, however, these findings seem to indicate that the randkluft governs the interaction between a cooler rock mass and a warmer ice mass.

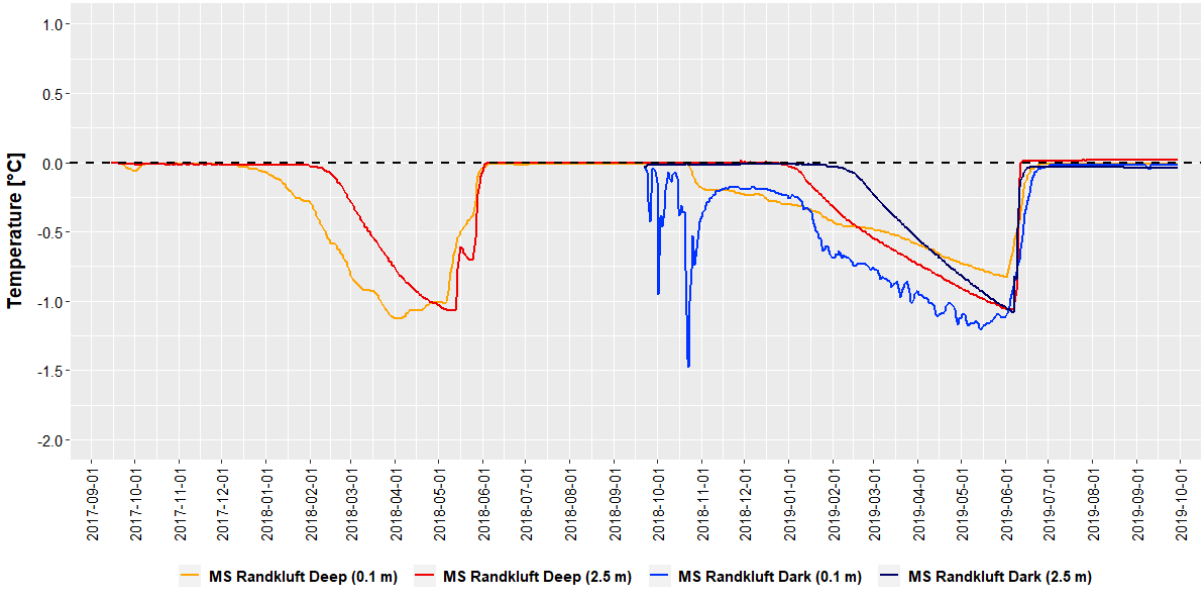

Figure 9: Recorded ice temperature at MS Randkluft Deep and MS Randkluft Dark for the two-year period Sep 2017 to Oct 2019. Sensor depth is given in brackets. Temperature at 0.1 m (MS Randkluft Dark) is significantly influenced by ventilation effects (e.g. cold air advection).

At MS Glacier a significant warming of the mean ice temperature was recorded with increasing borehole depth (Table 1). Annual amplitudes were attenuated significantly with increasing depth, at 10 m near-isothermal conditions were recorded. The lowermost sensor (12 m) showed significant deviations from this uniform pattern. It therefore appears likely that the bottom of the borehole has connected with the randkluft and as result, the lowest sensor is influenced by the more volatile temperature regime of the randkluft.

Table 1: Two-year mean ice temperature at MS Glacier for the period Oct 2017 to Sep 2019.

Borehole Depth [m]	1	2	4	6	8	10	12
Mean Temperature [°C]	-1.3	-1.0	-0.6	-0.4	-0.2	-0.1	-0.2

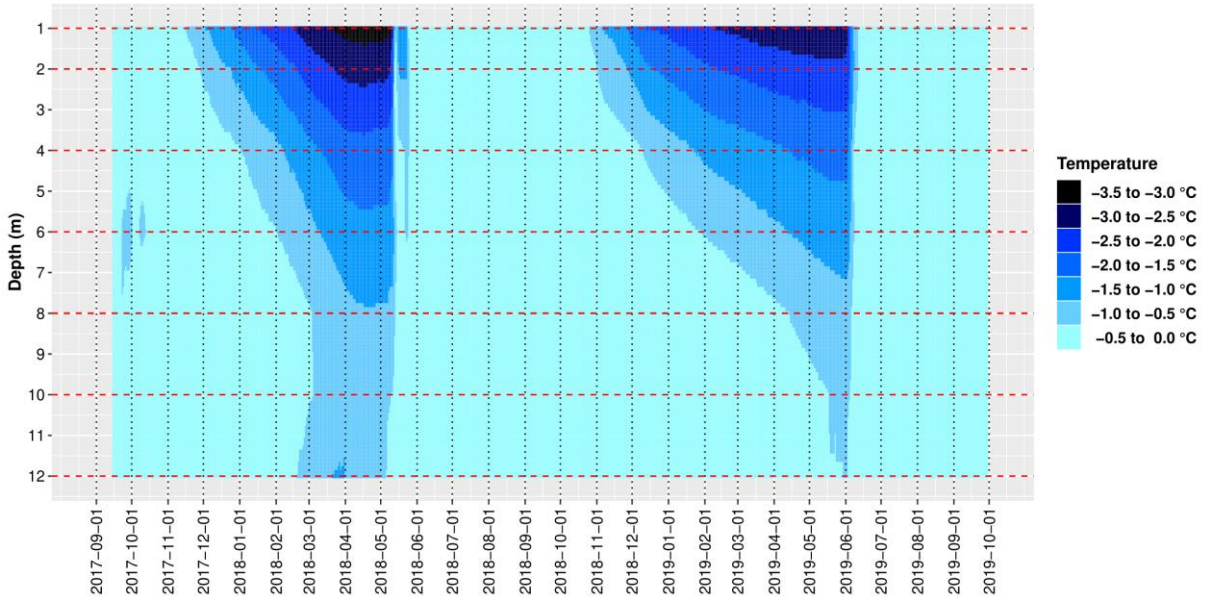

Figure 10: Ice temperature at MS Glacier for the period Oct 2017 to Sep 2019. The pronounced rapid temperature increase in late spring (early May 2018, early June 2019) is likely caused by intense latent heating during the refreezing of meltwater at the glacier surface or within the ice mass.

Surface cooling starts in October/November, low temperatures then uniformly penetrate into the ice mass (Figure 10). In late spring (May/June) a sharp, rapid warming is recorded at all depths, which establishes near-isothermal temperatures close to 0 °C across the entire vertical profile. Within this process, the cold wave from the previous winter is completely eradicated even at large depth. The warming period in 2018 was succeeded by a period of cold weather in May (one week) which caused short-term cooling before temperatures again rapidly rose to almost 0 °C. In 2019, warming was even more pronounced than in 2018 as temperatures across the entire borehole climbed to almost 0 °C within only two weeks.

The observed rapid warming of the ice mass in late spring is likely related to the ample supply of meltwater in this period. Liquid water from snow-melt is assumed to seep into the firn cover of the glacier where it is expected to refreeze and contribute to the formation of superimposed ice. During the refreezing process considerable amounts of energy are released, which then cause the observed pronounced warming.

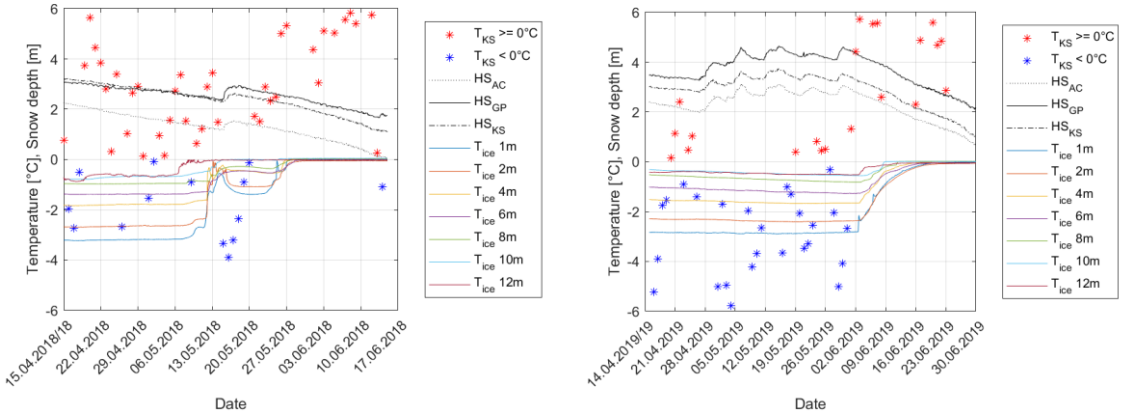

Figure 11: Rapid warming observed at MS Glacier in May 2018 (left) and June 2019 (right). Energy release during the refreezing of meltwater likely is the main driver behind the pronounced warming across the entire borehole profile. (T) Temperature, (HS) Snow Height, (AC) Weather Station Alpine Center (2445 m a.s.l.), (GP) Weather Station Gletscherplateau (2945 m a.s.l.), (KS) Weather Station Kammerscharte (2600 m a.s.l.)

A rough plausibility check underlines the potential significance of energy release during freezing. The melting of an assumed 0.2 m thick snow pack (density 400 kg/m³) leads to an energy release of 25 000 kJ/m², capable of warming a hypothetical 12 m ice column (1 m² base) by more than 1 °C. Snow depth records from nearby weather stations show significant snow melt (> 1 m in 2019) during the

pronounced warming period observed at MS Glacier (Figure 11). Rapid warming of the ice coincided with daily mean air temperatures exceeding 0°C. Thus, it can be assumed that no refreezing of meltwater in the already isothermal snow pack occurred and meltwater was routed efficiently to the snow-ice-interface where refreezing proceeded.
In 2018 the mean temperature of the ice column increased by 1.16°C within only eight days (6-14 May), which corresponds to a refreezing of a 0.08 m water head. This amount of meltwater corresponds to the melting of a 0.19 m thick snow pack, whereas observed snow depth decreased by 0.27 m in this period. In 2019 snow depth decreased by about 1.1 m from 3-17 June. A potential meltwater refreezing of 0.09 m water equivalent would have been sufficient to warm the total ice column by the observed 1.29°C.

3.3.3. Combined Simulation of Temperature Distribution

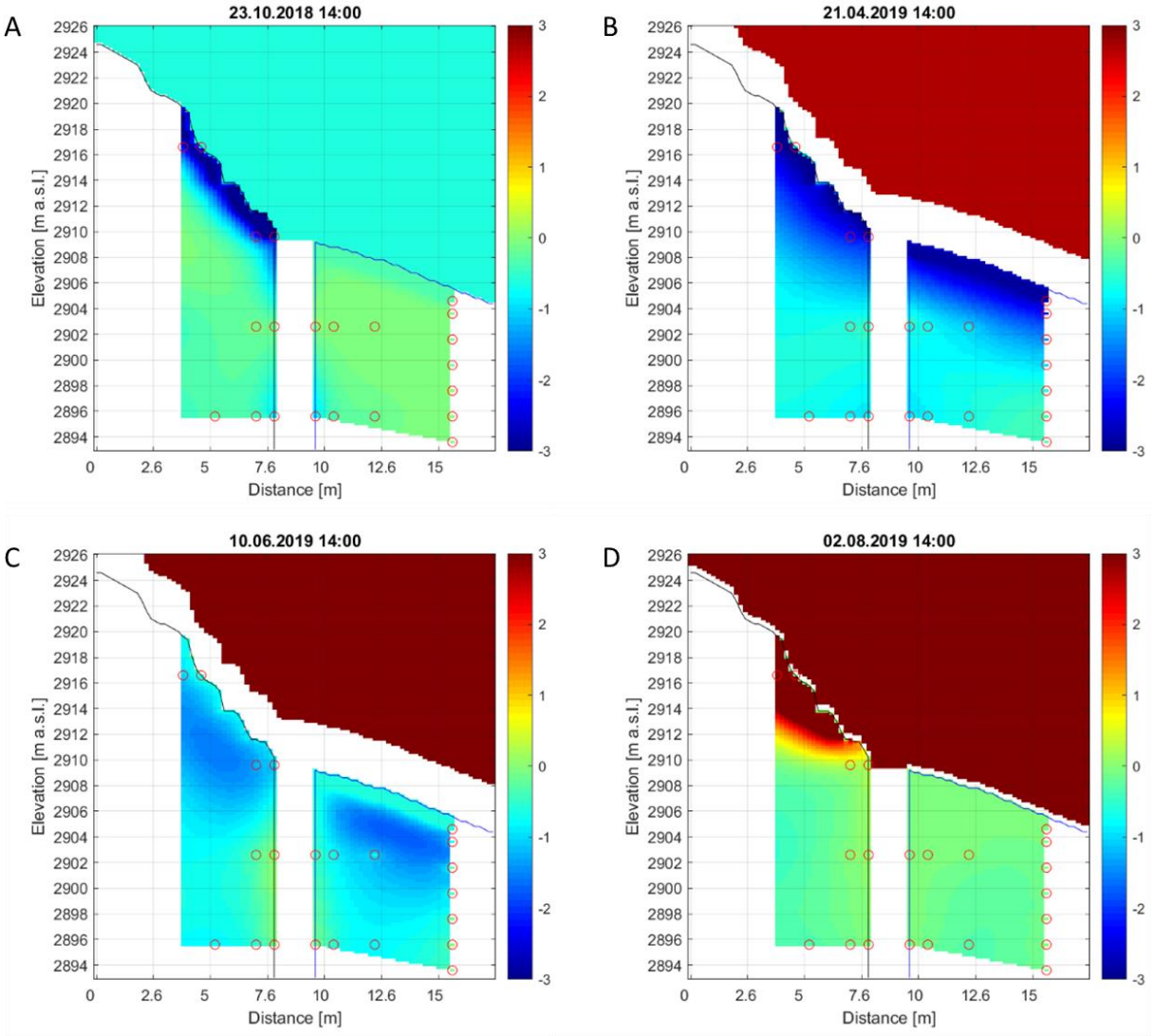

*Figure 12: Simulated 2D temperature distribution across the investigated glacier-headwall-interface (left side: headwall, right side: glacier). (**A**) Autumn: rapid near-surface freezing of the rock mass contrasts with slow cooling of the ice mass; (**B**) Winter: glacier and headwall show similar temperature distribution in late winter; (**C**) Spring: Terrain surface temperatures are still lower than temperatures inside the randkluft. The simulation (which is based solely on heat conduction) is unable to accurately represent the observed rapid warming of the ice mass induced by latent heating (compare to Figure 10); (D) Summer: Pronounced active layer formation in the rock mass, isothermal conditions slightly below 0 °C in the ice mass. Red circles symbolize location of temperature measurements.*

All available temperature measurements (bedrock and ice) where used as forcing input data for simulating the temperature distribution of the entire randkluft system. A complete energy balance

could not be simulated yet because of missing information on meteorological parameters inside the randkluft.
A 2D cross section was used for the simulation, covering the headwall, the randkluft and the glacier. High-resolution topography was derived from LiDAR and UAV data acquired within the project. Snow cover and air temperature outside the randkluft were estimated from nearby weather stations. The 7 m rock temperature from MS B2 was used as a boundary condition for deep rock temperature.
The simulation is not intended for detailed analyses since detailed structural geological conditions of the headwall and deep rock temperature at the glacier surface level are unknown. However, the simulation allows for a 3D interpretation of the temperature measurements. Due to its intuitive nature, it furthermore represents a valuable tool for research communication and transformation.
The simulation shows significant differences in cooling and warming between the rock and the ice section of the randkluft system. It emphasizes fast cooling of the rock and ice surface inside the Randkluft when cold air is advected through the randkluft opening in fall. Warming occurs as soon as the randkluft is snow-covered. After steady cooling over the winter months, rapid warming occurs in late spring, most likely caused by substantial energy release due to the refreezing of meltwater (see Chapter 3.3.2). Figure 12C highlights this drastic change in temperature diffusion when the observed rapid warming clearly outpaces simulated heat conduction within the ice volume.

Excursus: Temperature Monitoring at Randkluft Gefrorene Wand

Within the first year of the project, we got notice from an additional promising randkluft site below the west-face of the Gefrorene Wand peak in the Hintertux glacier resort (Tyrol, Austria). The commercially used randkluft/ice-cave system ('Eispalast') is reached by a narrow artificial entrance 15-20 meters below the glacier surface level at the contact zone between rock and glacier ice. After a horizontal distance of about 25 m a larger cave opened, where two rock temperature loggers at depths of 0.1 m and 0.8 m, one ice temperature logger at a depth of 0.1 m and one air temperature logger were installed on July 19th, 2017.
The recorded data show a constant but small offset of about 0.1 °C between air and ice temperature (Figure 13), which potentially indicates that the randkluft system (rock, air) is colder than the ice mass. Fast autumn cooling is evident in both years (September 2017, October 2018). At this time, the randkluft system was open to advection of cold air from the outside. As soon as the randkluft was closed and air circulation within the randkluft was halted, air and ice temperature increased again. During the ensuing winter cooling temperatures dropped to around -0.7 °C which were reached in early May 2018.

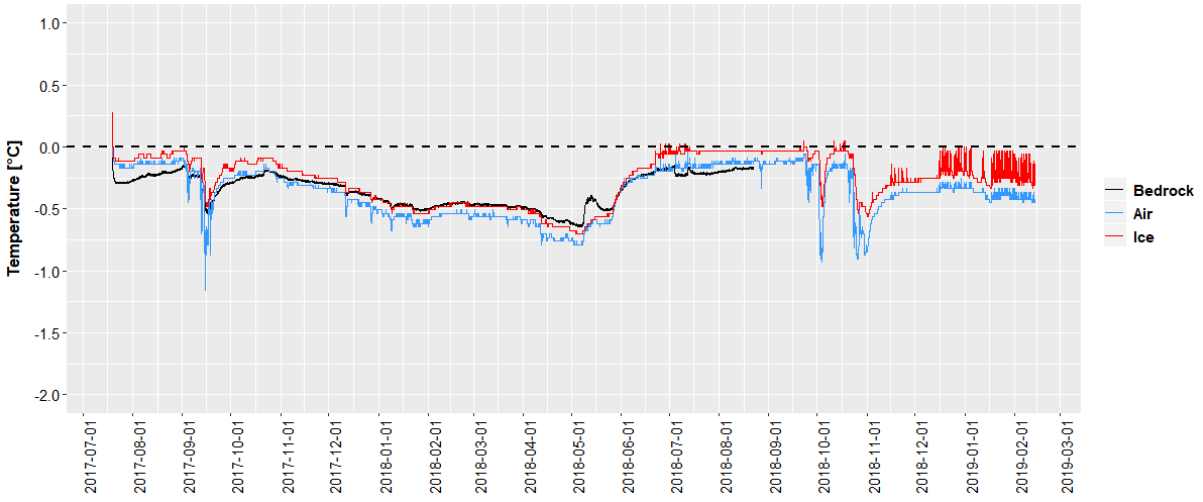

Figure 13: Bedrock, ice and air temperatures recorded at the randkluft below the Gefrorene Wand west-face (Tyrol, Austria). Bedrock and ice temperature was measured in 0.1 m deep boreholes.

Fast warming occurred at times of increased snow melt. In summer 2018, the ice temperature inside the randkluft stagnated at the melting point for nearly three months. Rock temperature on the contrary never reached the 0 °C plateau (lightning stroke destroyed the rock temperature logger by the end auf August).
Several negative temperature spikes probably induced by cold air advection were registered in autumn 2018. Temperatures in late autumn 2018 were higher than in the previous year potentially due to ventilation effects in the commercially used ice cave system. The observed spikes in air and ice temperature observed during the 2019 winter are daily cycles likely caused by intense illumination of the randkluft for exhibition purposes. Typical melt forms at the ice surface confirmed daily melting conditions even in winter time.

4. Rockfall Monitoring in Deglaciating Headwalls

Based on a six-year terrestrial LiDAR monitoring an extensive rockfall inventory was compiled and analyzed within the project. To this date the inventory represents the most extensive dataset on high-alpine rockfall worldwide and allows unprecedented insights into spatiotemporal rockfall patterns and their correlation with climate warming. Detailed results of the rockfall monitoring were recently published by Hartmeyer et al. 2020a and Hartmeyer et al. 2020b, excerpts are presented in the following sections.

4.1. Study Site Description

Two cirques immediately northwest of the Kitzsteinhorn summit were selected for rockwall monitoring. Both cirques are occupied by the Schmiedingerkees glacier, which is home to Austria's oldest glacier ski-area. All five rockwalls investigated tower above the Schmiedingerkees glacier: the Kitzsteinhorn north-face (KN), the Kitzsteinhorn northwest-face (KNW), the Magnetkoepfl east-face (MKE), the Magnetkoepfl west-face (MKW) and the Maurergrat east-face (MGE). The total surface area of all rockwalls studied is 234 700 m² and with an area of 133 400 m² and a mean height of roughly 200 m KNW is the largest rockwall studied. Slope gradients within and across the rockwalls vary greatly. Typically, gradients increase towards the glacier surface, as is characteristic for cirque walls worldwide (Benn & Evans 2010). With 72 ° the steepest mean gradient occurs at MKE, followed by MKW (63 °), and KNW displays the lowest gradient (44 °).

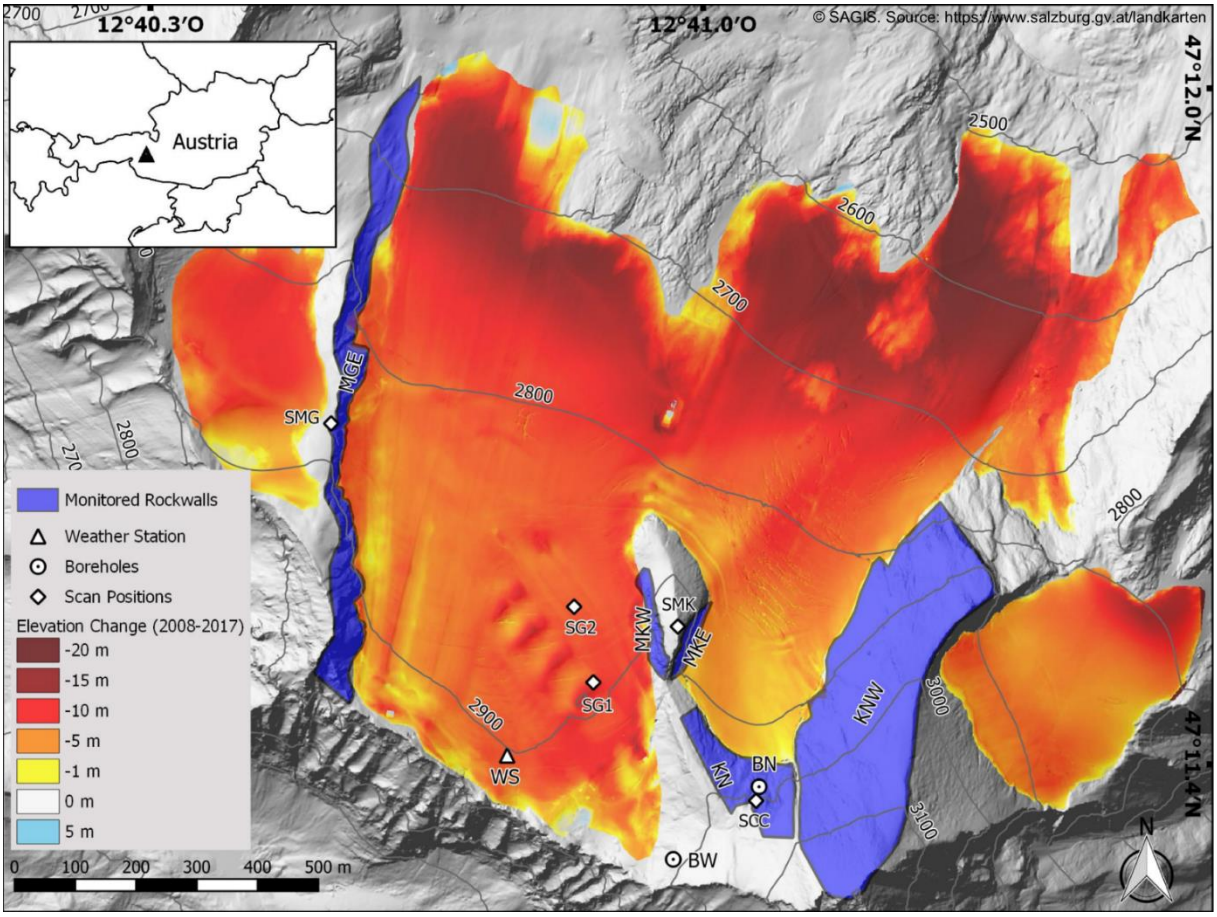

Figure 14: Hillshade of study area with monitored rockwalls, scan positions and elevation changes of the surface of the Schmiedingerkees glacier between 2008 and 2017. Abbreviations: K = Kitzsteinhorn (Summit), SMK = Scan Position 'Magnetkoepfl', SCC = Scan Position 'Cable Car Top Station', SG1 = Scan Position 'Glacier 1', SG2 = Scan Position 'Glacier 2', SMG = Scan Position 'Maurergrat', BN = Permafrost Borehole North-Face (30 m), BW = Permafrost Borehole West-Face (30 m).

The Schmiedingerkees glacier has retreated considerably in recent decades and ice-faces have degraded significantly in the surrounding cirque walls (Figure 14). The oldest useable aerial photos date back to 1953 (Land Salzburg 1953) and demonstrate a glacier area of 3.2 km². Since then the Schmiedingerkees glacier lost more than half of its size (-56 %) and the glaciated area decreased to 1.4 km² (2017). In 2008 the first comprehensive terrain data was acquired for the Schmiedingerkees (Land Salzburg 2008) using airborne laserscanning. The comparison with current UAV-derived terrain data demonstrates that in the period between 2008 and 2017 glacier volume decreased by 9.8 million m³. Mass loss was most pronounced near the terminus, but also in the root zone, i.e. adjacent to the rockwalls in focus here. Distinct ice-face degradation and glacier retreat is evident with annual surface lowering rates of around 0.5 m that exposed large, fresh bedrock surfaces (Figure 14).

4.2. Data Acquisition and Analysis

Terrestrial LiDAR data acquisition was performed using a Riegl LMS-Z620i laserscanner (Table 1). A calibrated high-resolution digital camera was mounted on the laserscanner for capturing referenced color images. First LiDAR data was acquired in July/August 2011 at all monitored rockwalls except MKW where data acquisition started in 2012. Data acquisition was restricted to the summer season (May to October). In total 78 rockwall scans were carried out from five different scan positions. Of these 22 scans were excluded from further analyses due to snow cover. Scan position 'Maurergrat' was abandoned in 2016, as due to continued glacial thinning site access was lost. Rockwall scans were repeated several times per summer season and at least once per season towards the end of the ablation period. The last scan of all rockwalls was carried out in August 2017, except for MKW that was excluded from further analysis, as unstable blocks were cleared away earlier in 2017 to reduce hazards for a new lift track.

Alignment of the acquired sequential point clouds was performed based on surface geometry matching within RiScanPro 1.8. First, point clouds were coarsely registered using the GPS location of the scan position and the azimuth angle of the laserscanner. Fine registration was performed with the ICP-algorithm, a popular cloud matching technique for finding the transformation between two point clouds by minimizing the square errors between corresponding entities. Consistent with previous studies on rock slope systems (Rosser et al. 2007, Abellán et al. 2011), alignment errors were negligible and typically ranged between 1 and 2 cm.

To identify surface changes in successive point clouds the M3C2 algorithm was used, which was specifically designed for orthogonal distance measurement in complex terrain (Lague et al. 2013). During the analysis, surface normal orientation is measured at a scale consistent with the local surface roughness and mean surface change is calculated along the normal direction.

Volumes of detached rock were derived from the distance calculations by identifying source areas, creating local grids and by subsequent grid-cell aggregation. Uncertainties in distance data were propagated using Gaussian error propagation to compute overall uncertainties. In addition, following parameters were determined for each source area: mean slope aspect and gradient, elevation above glacier surface as well as maximum depth of rock detachment (determined as the maximum Euclidean nearest-neighbor distance between the pre-event and the post-event point cloud).

4.3. Rockfall Inventory

During the six-year monitoring period (2011-2017) 632 rockfalls were registered with a total volume of 2 564.3 ± 1.5 m³. When omitting rockfalls below an uncertainty threshold of 0.1 m³, the total number drops to 374, while the overall volume is reduced only marginally to 2 551.4 ± 1.3 m³.

Large rockfalls over 100 m³ are rare (n = 5) but account for more than two thirds (68.5 %) of the total volume. The largest registered rockfall has a volume of 879.4 m³, the volumes of the three next largest

rockfalls range between 200-300 m³. With increasing volume an exponential decrease in number of rockfalls can be observed. Small rockfalls below 1 m³ represent 80 % of the total number but account for only 3.7 % of the overall rockfall volume.
Frontal photographs of the monitored rockwalls are provided in Figure 15. The source areas and rockfall volumes (> 0.1 m³) indicate that pre-existing weaknesses exert a strong control on rockfall occurrence. Concentration of rockfalls around fracture systems is particularly evident at KN (along cleavage planes) and KNW (along a prominent fault across the entire rockwall). The highest number of rockfalls was found at the largest rockwall KNW (n = 179). Lowest rockfall numbers were recorded at the smallest rockwalls at Magnetkoepfl (MKE, MKW). By far the highest total rockfall volume (1 455.4 ± 0.2 m³) was found at KN despite its relatively small size. Three of the five largest rockfalls occurred here. The second highest total volume was detected at KNW (541.2 ± 0.6 m³), while the lowest volume was recorded at MGE (125.5 ± 0.2 m³).

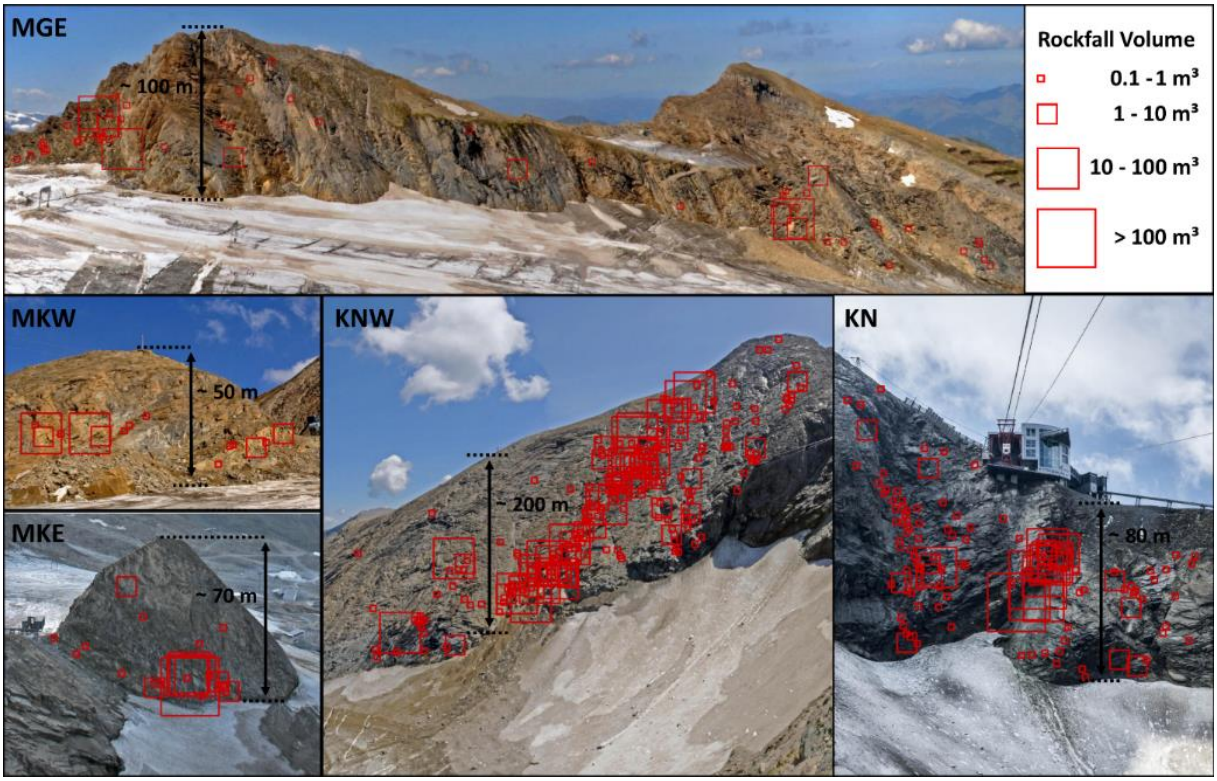

Figure 15: Rockfall source areas and volumes for all five monitored rockwalls.

4.4. Spatial Rockfall Distribution

To detail the vertical distribution of rockfall source areas, the elevation differences between rockfall source areas and local glacier surface are calculated and grouped into 10 m bins (Figure 16a). Immediately above the glacier surface (0-10 m) rockfall volumes are by far the highest (75.6 m³ per 10 000 m² a^{-1}) (Figure 16a). 60 % of the total rockfall volume detached from this segment, which constitutes only 15 % of the total rockwall surface area. With increasing distance from the glacier surface, a sharp decrease in rockfall volume can be observed. In the next higher segment (10-20 m), normalized rockfall volume slightly exceeds 20 m³ per 10 000 m² a^{-1}, while in all other height classes rates remain below 10 m³ per 10 000 m² a^{-1}. Only in two segments (90-100 m, 170-180 m), this pattern is masked by the presence of comparatively large, singular rockfalls.
Analyzed individually, a positive correlation between rockfall volume and proximity to glacier surface occurs for all rockwalls except KNW. The vast majority of the rockfall volume is detected within 10 m of the glacier surface at MGE (73 %), KN (79 %) and MKE (98 %). Considering the first 20 m above glacier surface the volume percentages exceed 90 % for all three rockwalls.

At MKW rockfall volumes are small in the lowest segment (3 %) and 96 % of the rockfall volume occur in the segment above (10-20 m). Here, a rockfall event from the early 2000s, created a steep scarp around 15 m above the current glacier surface. The rockfall deposits, likely several thousand cubic meters of rock, accumulated at the foot of MKW and constituted a talus cone that decoupled parts of the rockwall from the glacier. The rockfall scarp remained a prominent source area for rockfall during the monitoring period, indicating continued stress release after the initial event. Rockfall from this scarp was the main reason why this rockwall displays a differing pattern and maximum retreat rate does not occur within the first ten vertical meters above glacier surface.

As mentioned no pronounced glacial proximity pattern was found for KNW, where only 12 % of the rockfall volume detached within the first 10 m. Here, a significant 272.7 ± 0.03 m³ rockfall occurred in summer 2016 which constituted around half of the total rockfall volume at this site. Its rockfall source area is located 97 m above the glacier surface and may coincide with the LGM trim line. Still, after excluding this event, only a rather weak proximity pattern is observed (23 % of the volume within the lowest 10 m) clearly deviating from the patterns observed at the other four rockwalls.

Analysis of rockfall numbers confirms the glacial proximity pattern even though the correlation is much less pronounced than for the elevation volume distribution. Highest normalized rockfall numbers (3.9 rockfalls per 10 000 m^2 a^{-1}) are once again found in the lowest segment (0-10 m) (Figure 16c). The mean value for all higher segments (i.e. 10-260 m) equals 2.5 rockfalls per 10 000 m^2 a^{-1} with significant variations between the different height classes. Overall 21 % of all rockfalls occurred in the first 10 m above the glacier surface – a distinct contrast to the dominance of rockfall volumes in that segment.

Comparing rockfall numbers across the rockwalls yields diverse results: At KN particularly high rockfall numbers are found between 30 and 50 m above the glacier. KNW shows a more uniform pattern with a rather balanced distribution over the first 100 m and a slight decrease at higher elevations. At MKE, rockfall is restricted to the immediate adjacency to the glacier and above the 0-10m-segment only minimal rockfall activity is observed. At MKW and MGE, most rockfalls occurred within 20 m of the glacier surface (ca. 70 % and 90 %, respectively).

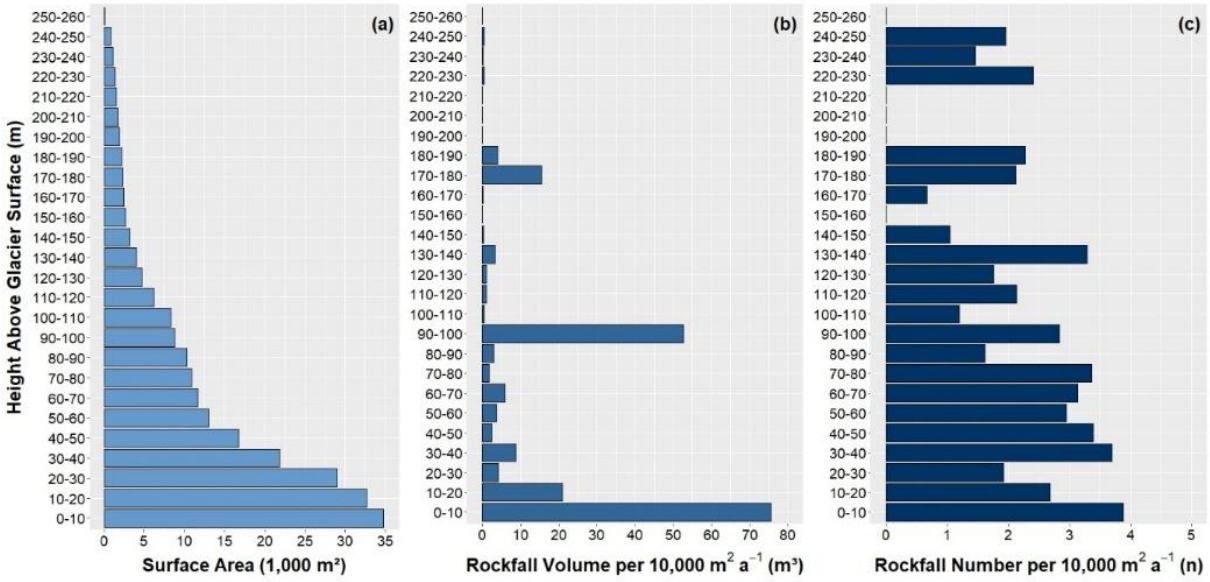

Figure 16: (a) Rockwall surface area, (b) normalized rockfall volume and (c) the normalized number of rockfalls, classified by elevation above glacier surface. Areas exposed by recent glacier retreat are heavily susceptible to rockfall, during the observation period (2011-2017) 60 % of the total rockfall volume detached within 10 m of the current glacier surface.

4.5. Antecedent Rockfall Preparation inside the Randkluft

Slope debuttressing following deglaciation is frequently considered to cause mass movements, particularly in case of larger slope failures. (e.g. Holm et al. 2004, Allen et al. 2010). At the base of the

investigated rockwalls, however, seasonally air- or snow-filled voids between glacier and cirque wall ('randkluft') prevent permanent physical contact between rock and ice and thus effectively hinder debuttressing. The existence of a randkluft is not site-specific but rather common at alpine (cirque) glaciers (e.g. Gardner 1987, Mair & Kuhn 1994, Sanders et al. 2012). Among the rockwalls investigated here, randkluft systems are most pronounced below KN, possibly due to the principal flow direction of the adjacent glacier perpendicularly away from the slope. Randkluft development is rather limited at KNW, likely caused by substantial (avalanche) snow accumulation at the foot of the tall, low-gradient rockwall.

Local randkluft systems at the Kitzsteinhorn are usually open during late summer/early fall, even though randkluft width and depth exhibit considerable interannual variations. It is evident from our observations that the debuttressing effect, if relevant at all (McColl & Davies 2012), can occur subglacially only, in the lowermost parts of the randkluft. Sporadically, the collapse of ice bridges may cause small-scale debuttressing locally, but in general this mode of failure seems not too effective. Debuttressing can also not explain the increased rockfall activity several meters above the glacier surface, i.e. in areas already ice-free for years or decades.

Previous modelling approaches assume unfrozen conditions for currently glacier-covered, north-facing headwall sections and aggradation of new permafrost after deglaciation (Wegmann et al. 1998). Other studies report distinct permafrost conditions inside randkluft systems based on in-situ temperature measurements (Sanders et al. 2012). Our observations match with the latter findings, as we encountered rockwalls coated with refrozen meltwater ('verglas') as deep as 15 m below the glacier surface during late summer. The existence of perennially frozen conditions inside the randkluft combined with observed extensive meltwater supply from the rockwall above may significantly contribute to the efficacy of frost weathering in subglacial cirque wall sections. One of the few quantitative studies indicates particularly effective rock-fracturing driven by ice segregation within the randkluft of a temperate glacier in British Columbia, Canada (Sanders et al. 2012). This observation has recently been substantiated by numerous field and lab experiments demonstrating intense frost cracking at temperatures just below 0 °C (Girard et al. 2013, Duca et al. 2014, Murton et al. 2016) and thermo-cryogenic rock fatigue due to damage accumulation over longer time scales (Jia et al. 2015). Subcritical stress propagation driven by sustained freezing and sufficient water supply (Jia et al. 2017, Draebing & Krautblatter 2019), and high plucking-related tensile stresses caused by refreezing meltwater at the bottom of the randkluft (Lewis 1938, Hooke 1991). We hypothesize, therefore, that they are the dominant antecedent processes of rockfall preparation. The special weathering conditions may prepare the high fragmentation of near-randkluft bedrock which efficiently predisposes cirque walls to shallow failures and ultimately controls the high post-glacial rockfall activity. This idea is further underpinned by a possible positive correlation between randkluft size and glacier-proximal rockfall volume. Highest proximal rockfall volumes are found at KN and MKE which also host the largest randkluft systems of all rockwalls monitored. Lowest proximal rockfall volumes are recorded at KNW where randkluft formation is suppressed due to massive local snow accumulation at the glacier fringe.

4.6. Deglaciation-Induced Thermomechanical Forcing and Active Layer Formation

As glaciers are wasting down, freshly exposed rockwall sections are shifted from subglacial to subaerial boundary conditions. The quantitative effects of this transition are elusive, as direct measurements from subglacial cirque wall sections are rare (Gardner 1987, Sanders et al. 2012). Yet it is expected that thermal conditions in cirque walls are modified significantly as they emerge from isothermal, subglacial conditions – a transition that has recently been named 'paraglacial thermal shock' (Grämiger et al. 2018). Once ice-free, strong diurnal and seasonal variations are likely to induce pronounced thermal stress leading to deformation (Hasler et al. 2012, Weber et al. 2017) and potentially to failure along critically-stressed discontinuities (Hall 1999, Gischig et al. 2011). Additionally, cyclic freeze-thaw action

will cause rock fatigue (Jia et al. 2015), hydrofracture (Davidson & Nye 1985, Sass 2004) and the expansion of water-filled joints (Matsuoka & Murton 2008), all of which promote destabilization in recently deglaciated rockwall sections (Draebing et al. 2017).
Active layer deepening – a key element of permafrost degradation (Ravanel et al. 2017) – significantly alters rock- and ice-mechanical properties (Davies et al. 2001, Krautblatter et al. 2013) and is frequently considered in high-alpine rockfall analyses (e.g. Gruber & Haeberli 2007, Weber et al. 2019). Failure depth of rockfalls related to permafrost degradation is expected to equal or exceed maximum active layer thickness. At a local borehole monitoring site at KN the active layer depth varies between 3-4 m inter-annually. Based on these values, only 0.5 % (below 4 m) to 1.3 % (below 3 m) of all rockfalls failed at a depth below the maximum seasonal active layer. Volume shares are significantly higher due to the large size of the deeper-seated events: Rockfalls with failure depths larger than 3 m (4 m) constitute 44 % (60 %) of the total rockfall volume, suggesting that permafrost degradation could indeed have a substantial impact on total rockfall volume.
Active layer thickness is expected to vary strongly across the investigated rockwalls (Schrott et al. 2012), mainly due to topography effects (Gruber et al. 2004) and snow cover variations (Haberkorn et al. 2015). Active layer depth monitored at KN is therefore unlikely to be representative for the entire study area. Particularly for recently deglaciated rockwall sections, permafrost dynamics are poorly understood due to the complex local interplay of glaciological, meteorological and geological controls (Draebing et al. 2014). Observations point at the complete absence of an active layer in glacier-covered rockwall sections. Glacial downwasting would thus uncover permanently frozen rockwalls and cause the formation of an incipient active layer. This process is expected to have a significant destabilizing effect (Davies et al. 2001, Krautblatter et al. 2013) and may therefore contribute considerably to the increased rockfall activity near the current glacier surface.

4.7. Conclusions

The compiled inventory represents the most extensive dataset of high-alpine rockfall to date and the first quantitative documentation of a cirque-wide erosional response of glaciated rockwalls to recent climate warming. Rockfall activity concentrates along pre-existing structural weaknesses and was highest in recently deglaciated areas: 60 % of the rockfall volume originated from source areas located fewer than ten vertical meters above the current glacier surface, 75 % detached within 20 vertical meters of the glacier surface. Increased mass wasting activity in recently deglaciated areas, such as discovered in the present study, is typical of paraglacial environments, where slope systems gravitationally adjust to new, non-glacial boundary conditions. Distinct randklufts, which separate the investigated cirque walls from the adjacent glacial ice, effectively prevent debuttressing. Inside the randkluft we observed perennially frozen conditions and extensive refreezing of meltwater supplied from the rockwall above. Sustained freezing along with sufficient water availability in the randkluft likely drive subcritical stress propagation and cause high plucking-related tensile stresses, which contribute to antecedent rockfall preparation when the rockwall is still ice-covered. As the glacier is wasting down strong diurnal and seasonal temperature variations induce pronounced thermal stress, cause rock fatigue and lead to the first-time formation of an active layer, which is expected to exert a significant destabilizing effect on glacier-proximal areas.

5. Semi-Automatic Identification of Glacier Headwalls on a Regional Scale

The European Alps might be ice-free by the end of this century (Zekollari et al. 2019), raising the need to anticipate future glacially induced rock slope instabilities rather than study them in retrospect. Despite a large number of studies on glacier-induced rock slope instabilities (e.g. Ballantyne et al. 2014), a systematic regional-scale identification of the rockfall source area, the glacier headwall, is absent. A first approach to identify glacier headwalls semi-automatically is presented here. This part of the *GlacierRocks* project aims to

(i) identify glacier headwalls on a regional scale using semi-automatic techniques, and
(ii) locate recently and potential future deglaciated headwalls.

The presented study offers a new and unique dataset on the regional distribution of recently deglaciated and current potentially unstable rock slopes as well as on rock slopes that may become unstable after being deglaciated in the near future.

5.1. Material and Methods

We performed the study within the boundaries of the Hohe Tauern Range, which includes the study site Kitzsteinhorn and encompasses the mountain ranges of Venediger-, Granatspitz-, Glockner-, Goldberg- and Ankogelgruppe. We used a DEM with a 10 m resolution and glacier outlines from 1850 and 2015 compiled in the Austrian Glacier Inventory (Fischer et al. 2015, Buckel & Otto 2018) as base data.
Semi-automatic headwall detection used object-based image analysis techniques (OBIA) with the eCognition Developer 9. Segmentation is based on the DEM, the additional DEM derivatives slope and aspect, and a TPI-based (Topographic Positioning Index) landform classification (Weiss 2001). Segmentation parameters are summarized in Table 2. Automated classification of headwall objects was based on the following criteria: mean slope was >= 35° (Evans & Cox 1974) and minimum elevation >= 1500 m a.s.l.. The definition of classification criteria aimed at excluding objects at elevations below glacier occurrence, which may be shaped by non-glacial processes. For validation, headwalls within a subset of the study area were mapped using digital aerial orthophotos and additional maps of hillshade and slope angle. Headwall mapping is based on existing definitions including slope area of > 35° and lower and upper boundaries represented by schrundline/glacier margin and ridges, respectively. Schrundlines are distinct breaks in slope that manifest headwall erosion at long-term locations of the Randkluft/Bergschrund at the upper glacier boundary. Semi-automatically identified headwalls were then compared to manually mapped headwalls to assess the quality of the OBIA approach.

Table 2: Segmentation parameters used for semi-automatic headwall detection.

Segmentation	
Parameter	Value
Image layer weights	
Aspect	1
TPI	2
Slope	4
Scale Parameter	65
Shape	0.1
Compactness	0.8

In order to identify deglaciated headwalls we intersected headwall polygons with areas released by glacier melt between 1850 and 2015. Intersecting the headwall polygons with the 2015 glacier extent delivers the parts of the headwalls that are still under ice cover today.

5.2. Results and Interpretation

The semi-automatic approach delivered an area of 636 km² classified as potential headwalls (Figure 17). Within the subset for validation, objects with a total area of 108 km² were generated. In comparison, a headwall area of around 49 km² was mapped manually representing 45% of overlap between the two approaches. Consequently, 55% of the area semi-automatically mapped represented non-headwall slope situations. However, overlapping areas contain most of the slopes near glaciers that have been interpreted as headwalls. The overestimation shows that the chosen segmentation and classification approach is not fully capable of producing only objects that are interpreted as headwalls. This disparity may arise from differences in identification criteria between the subjective manual mapping and the semi-automatic approach. Manual mapping considered the glacier extents and schrundlines for landform identification. Glacier extents have not been considered, since we aimed at also identifying headwalls in completely ice-free cirques. We assume that the OBIA approach could be improved taking into account more topographic characteristics, like the location of schrundlines to better distinguish between headwalls and other slope locations. The method is currently refined to generate data sets of schrundlines for the study area. One characteristic of schrundlines is a distinct break in slope, which could be identified using profile curvature analysis. However, some headwalls are not marked by distinct schrundlines or once existing schrundlines might have been eroded rapidly after deglaciation.

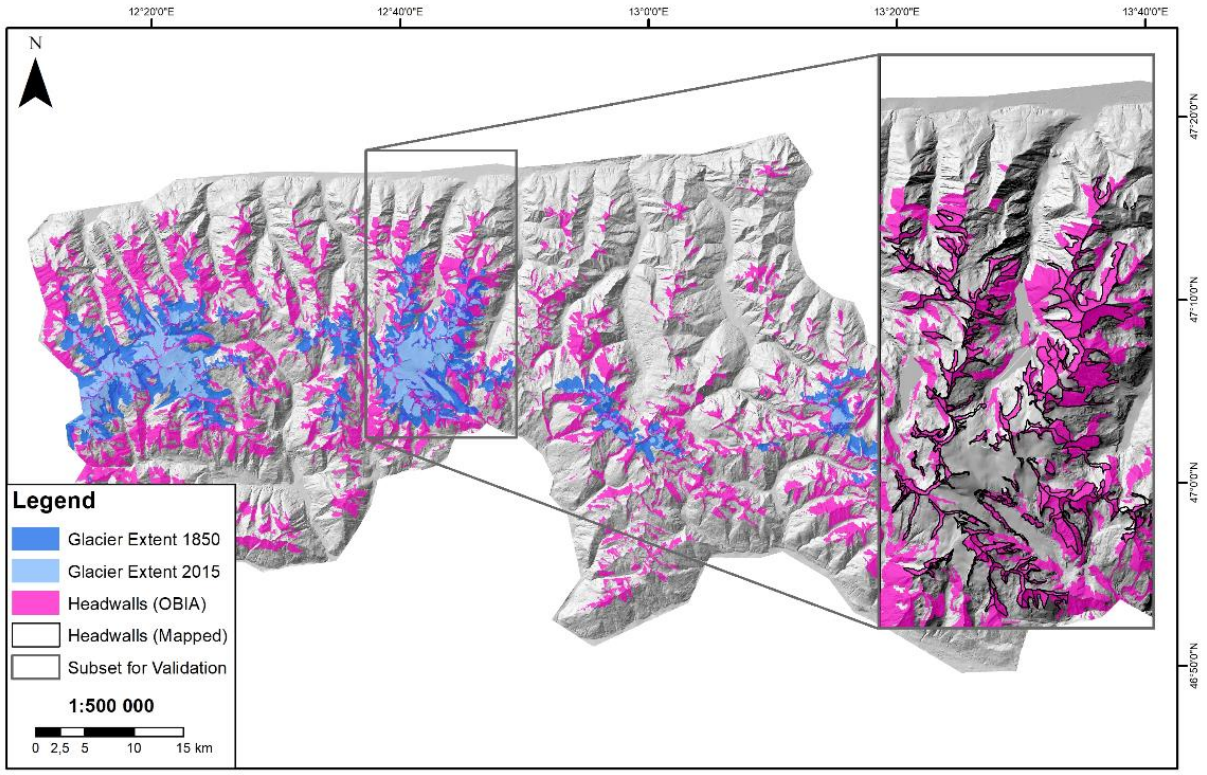

Figure 17: Results of semi-automatic headwall delineation for the Hohe Tauern area. The subset shows a comparison of manually and semi-automatically mapped headwalls.

Despite overestimation of the semi-automated approach, the results cover most of the existing headwalls near the glacier. This allowed us to quantify headwall areas, which have been deglaciated in the recent past or will potentially be released by future glacier melt. An area of 202 km² of terrain was released by glacier retreat between 1850 and 2015 in the Hohe Tauern Range. We identified an area of 36 km² (17 %) as glacier headwalls (red areas in Figure 18). Our results show that underneath the remaining glacier area in 2015 (118 km²) an area of 11 km² belong to glacier headwalls and subglacial steep parts at cirque outlets (blue areas in Figure 18). A close-up of the Glockner Massif

(Figure 18), demonstrates that large parts of the headwalls have been deglaciated. Additional areas of headwalls will be uncovered in the future leading to a significant increase of steep slopes. However, since the ice-covered headwalls were estimated from the slope angle of the glacier uncertainties may arise if the glacier topography differs significantly from the subglacial topography.

Considering an increased potential for destabilization in deglaciated terrain (e.g. Hartmeyer et al. 2020a), the presented approach is able to quickly identify locations and extents of headwall deglaciation and therefore contributes to an improved anticipation of potential instabilities. A future integration of stability-relevant parameters (e.g. rock mechanical parameters, thermal state) into the presented regional-scale approach could result in a regional risk analysis tool for high-alpine infrastructure planning. This part of the project will be continued within the ÖAW-DOC project RIDGES by Andreas Ewald at the University of Salzburg.

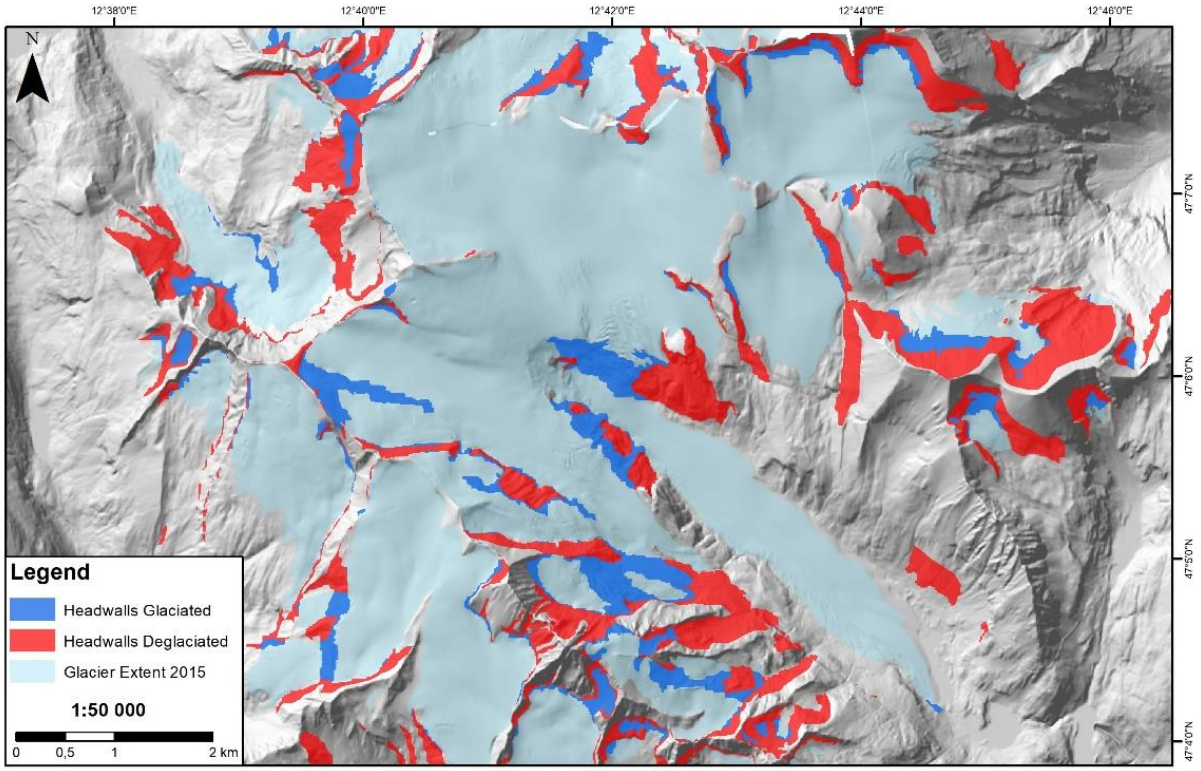

Figure 18: Locations of headwalls that have been deglaciated since the LIA (red) or will be released by glacier melt in the future in the Großglockner area, derived from the semi-automatic analysis.

6. Microclimatic and Acoustic Emission Monitoring

To study microclimatic conditions in various randkluft depths, three miniature weather stations (Libelium Smart Agriculture Xtreme 1.0) were prepared and tested for field operation (Figure 19A). The weather stations were equipped with sensors to monitor (i) air temperature, air humidity and atmospheric pressure (Bosch Sensortec BME280), (ii) the distance between glacier and headwall with an ultrasound sensor probe (I2CXL-MaxSonar-MB7040), (iii) solar radiation (SQ-110), (iv) rock moisture with a leaf wetness sensor (Decagon Phytos 31), and (v) wind direction and speed with a sonic anemometer (Decagon DS-2). The weather stations are powered by 4V batteries, the recorded data is transmitted via cellular network, which is of excellent quality at the study site even at MS Randkluft Dark (15 m below the glacier surface) (Figure 19B+C).
Extensive operability tests were carried out during the 2018 and 2019 field season. However, continuous long-term monitoring has so far proved unsuccessful. Installation of equipment and required utilities (energy supply) proved to be more difficult and labor intensive than estimated leading to significant delays and maintenance issues. Further tests which hopefully will pave the way for a successful long-term monitoring of microclimatic conditions inside and above the randkluft are planned for the upcoming 2020 field season.

*Figure 19: (**A**) Assembling tests of miniature weather station (Libelium Smart Agriculture Xtreme 1.0) connected to all five sensors; (**B**) Weather station installed at MS Randkluft Dark inside a robust aluminum housing (1), connected to external 4V battery (2) and external antenna (3); (**C**) Weather station covered with thin layer of ice ('verglas') after a one-year test run inside the randkluft (MS Randkluft Dark).*

Bedrock fracturing by frost weathering is considered one of the key controls on long-term headwall evolution and rockfall preparation (e.g. Scherler 2014, Sanders et al. 2012). However, little is known on its efficacy in glacial headwalls let alone inside randkluft systems. To investigate near-surface bedrock fracturing (micro cracking) at decimeter-scale cracks an acoustic emission (AE) monitoring was installed. The AE system consists of a rugged miniature PC (Fitlet RM iA10), four acoustic emission nodes (Mistras 1283 USB AE Node) and four narrowband, high-sensitivity sensors (Mistras R6I-UC Sensor) (Figure 20A).
The AE system was installed at MS Randkluft Lip to test its operability under high-alpine conditions. To supply the AE system with electricity a power line was installed across the entire rockwall. The field computer and the AE nodes were placed inside a robust aluminum box (Zarges), which was installed a few meters from the measurement site. The rock surface at the measurement site was grinded with a grinding machine to ensure optimal coupling between the AE sensors and the rockwall (Figure 20A). Unfortunately heavy snow pressure at the measurement site caused severe damage to the installation and has so far prevented long-term monitoring (Figure 20B). In the upcoming field season further tests will be carried out to facilitate a safe and successful future application.

Figure 20: (A) Acoustic emission (AE) sensors (Mistras R6I-UC Sensor) installed directly at the randkluft opening (MS Randkluft Lip); (B) Aluminum box immediately above the AE monitoring twisted by snow pressure.

7. Outlook

Models suggest a temperature increase of 1.5 °C over the next 30 years in Austria (APCC 2014), which will further accelerate the dramatic retreat of glaciers currently observed. By the end of the century glaciers in Austria are expected to decrease to less than 20 % of today's area (Zemp et al. 2006). Deglaciation will therefore continue to alter the face of the Alps and elevated rockfall from freshly exposed rockwalls – quantified systematically in this project for the first time ever (Hartmeyer et al. 2020a, Hartmeyer et al. 2020b) – will be of growing relevance for stakeholders, practitioners and scientists.

Within the present study a unique monitoring of rock and ice temperature was established inside and above a randkluft. Measurements were carried out up to 15 m below the current glacier surface. Due to highly challenging accessibility and harsh environmental conditions no comparable monitoring exists to this date. After the conclusion of the project the randkluft monitoring will be integrated into the research infrastructure of the Open-Air-Lab Kitzsteinhorn, which will enable long-term continuation of all monitoring activities initiated within *GlacierRocks*.

Perennial monitoring is of essential significance to systematically identify and characterize the impacts of atmospheric warming, which often show considerable lag times and may become visible only on multi-decadal time-scales. Assuming continued glacial thinning the randkluft-monitoring established in the present study will be exhumed from the depths of the randkluft over the next years and decades. The installed instruments are therefore in a prime position to observe the transition from isothermal subglacial conditions to highly variable conditions governed by the atmosphere at first hand. The data acquired in the process will substantially deepen the understanding of the thermal dynamics at the glacier-headwall-interface. The results will furthermore help our understanding of destabilization and increasing rockfall hazards in deglaciating headwalls and will therefore contribute to improved climate change adaptation strategies and infrastructure safeguarding in high-alpine glacial environments.

8. Publications (Project Output)

Peer-reviewed Publications

Hartmeyer, I., Delleske, R., Keuschnig, M., Krautblatter, M., Lang, A., Schrott, L., and Otto, J.-C.: Current glacier recession causes significant rockfall increase: The immediate paraglacial response of deglaciating cirque walls, Earth Surface Dynamics Discussion, 2020a. [Weblink]

Hartmeyer, I., Keuschnig, M., Delleske, R., Krautblatter, M., Lang, A., Schrott, L., and Otto, J.-C.: Enhanced rockwall retreat and modified rockfall magnitudes/frequencies in deglaciating cirques from a 6-year LiDAR monitoring, Earth Surface Dynamics Discussion, 2020b. [Weblink]

Media Activities

Am Seil die Gletscherkluft erforschen. Die Presse, 01.07.2017, Page 26. [Weblink]

Alerte Glaciers, TV Documentary for 'Sciences & Vie', 52 minutes, Producer: Thibault Ferié, broadcast 18.02.2020. [Weblink]

Academic Theses

Ewald, A.: Fracture Dynamics and Rock Slope Stability in Deglaciating Headwall Systems, Diploma Thesis, University of Salzburg, 55 pp., 2018.

Hartmeyer I.: Destabilization and rockfall in deglaciating, permafrost-affected cirques, PhD Thesis, University of Salzburg, in preparation.

Contributions in Conference Proceedings

Hartmeyer, I., Keuschnig, M., Krautblatter, M., Helfricht, K., Otto J.-C., and Leith K.: Glacial Thinning and its Influence on Rockfall Activity: Introducing a new high-alpine Monitoring Site. Poster presentation at EGU General Assembly 2017, Vienna, Austria, Geophysical Research Abstracts Vol. 19, EGU2017-14921, 2017. [Weblink]

Keuschnig, M. and Hartmeyer, I.: The Open Air Lab Kitzsteinhorn (OpAL) – Open Innovation in High Altitude. Poster presentation at 6th International Symposium for Research in Protected Areas 2017, Salzburg, Austria, 2017. [Weblink]

Hartmeyer, I., Keuschnig, M., Fegerl, L., Valentin, G., Helfricht, K., and Otto, J.-C.: Long-term monitoring of climate-sensitive cirques in the Hohe Tauern range. Talk at 6th International Symposium for Research in Protected Areas 2017, Salzburg, Austria, 2017. [Weblink]

Helfricht, K., Hartmeyer, I., Keuschnig, M., Krautblatter, M., Leith, K., and Otto, J.-C.: Microclimate and temperature distribution inside a randkluft system – first observations and insights. Poster Presentation at EMS Annual Meeting 2019, Copenhagen, Denmark, Vol. 16, EMS2019-90, 2019 [Weblink]

Conference Presentations

Hartmeyer, I. and Keuschnig, M.: GlacierRocks - Glacier-Headwall Interaction and its Influence on Rockfall Activity. Talk at AK Permafrost 2017, 09.-11.02.2017, Einsiedeln, Switzerland, 2017.

Helfricht, K., Hartmeyer, I., Keuschnig, M., Krautblatter, K., Leith, K., and Otto, J.-C.: GlacierRocks - Wechselwirkungen zwischen Gletscher und Felswand in Randklüften und deren Auswirkungen auf die Steinschlag-Aktivität. Poster presentation at Jahrestagung des AK Hochgebirge, 2.-4. Februar 2018, Innsbruck, Austria, 2018.

Hartmeyer, I., Keuschnig, M., Helfricht, K., Leith, K., Otto, J.-C., and Krautblatter, M.: Thinning Glaciers, Falling Rocks? The intriguing (and unknown) contribution of recent glacier retreat to increased high-alpine rockfall activity. Poster presentation at 19th Austrian Climate Day, 23.-25. April 2018, Salzburg, Austria, 2018.

Hartmeyer, I., Keuschnig, M., Helfricht, K., Leith, K., Otto, J.-C., and Krautblatter M.: Thinning Glaciers, Falling Rocks? Recent glacier retreat and its contribution to increased high-alpine rockfall activity. Poster presentation at the 10th AK Permafrost 30. November - 2. December 2018, Bremerhaven, Germany, 2018.

9. List of Abbreviations

AE	Acoustic Emission
DEM	Digital Elevation Model
GIS	Geographic Information System
ICP	Iterative-Closest-Point
KN	Kitzsteinhorn north-face
KNW	Kitzsteinhorn northwest-face
LiDAR	Light Detection and Ranging
MGE	Maurergrat east-face
MKE	Magnetkoepfl east-face
MKW	Magnetkoepfl west-face
MS	Measurement Site
OBIA	Object-based Image Analysis
OPAL	Open-Air-Lab Kitzsteinhorn
TLS	Terrestrial Laserscanning
UAS/UAV	Unmanned Aerial System/Vehicle

References

Abellán, A., Vilaplana, J. M., Calvet, J., García-Sellés, D., and Asensio, E.: Rockfall monitoring by Terrestrial Laser Scanning – case study of the basaltic rock face at Castellfollit de la Roca (Catalonia, Spain), Natural Hazards and Earth System Sciences, 11(3), 829-841, 2011.

Allen, S. K., Cox, S. C., and Owens, I. F.: Rock avalanches and other landslides in the central Southern Alps of New Zealand: a regional study considering possible climate change impacts, Landslides, 8(1), 33-48, 2010.

ALPHAZ: Munich Alpine Hazards and Mitigation Cluster, 2020 [Online]. Available: https://www.bgu.tum.de/alphaz/news/ [Accessed 30.04.2020].

APCC – Austrian Panel on Climate Change: Österreichischer Sachstandsbericht Klimawandel 2014 (AAR14). Austrian Panel on Climate Change (APCC), Verlag der Österreichischen Akademie der Wissenschaften, Vienna, Austria, 1096 pp., 2014.

Ballantyne, C. K., Sandeman, G. F., Stone, J. O., and Wilson, P.: Rock-slope failure following Late Pleistocene deglaciation on tectonically stable mountainous terrain, Quaternary Science Reviews, 86, 144-157, 2014.

Benn, D. I. and Evans, D. J. A.: Glaciers & Glaciation, Routledge Taylor & Francis Group, London and New York, 2010.

Buckel, J. and Otto, J.-C.: The Austrian Glacier Inventory GI 4 (2015) in ArcGis (shapefile) format: Supplement to: Buckel, J., Otto, J.-C., Prasicek, G., and Keuschnig, M. (2018): Glacial lakes in Austria - Distribution and formation since the Little Ice Age. Global and Planetary Change, 164, 39-51, 2018.

Davidson, G. P. and Nye, J. F.: A photoelastic study of ice pressure in rock cracks, Cold Regions Science and Technology, 11(2), 141-153, 1985.

Davies, M. C. R., Hamza, O., and Harris, C.: The effect of rise in mean annual temperature on the stability of rock slopes containing ice-filled discontinuities, Permafrost and Periglacial Processes, 12(1), 137-144, 2001.

Deline, P., Gruber, S., Delaloye, R., Fischer, L., Geertsema, M., Giardino, M., Hasler, A., Kirkbride, M., Krautblatter, M., Magnin, F., McColl, S., Ravanel, L., & Schoeneich, P.: Ice loss and slope stability in high-mountain regions. In W. Haeberli, C. Whiteman, & J. F. Shroder (Eds.), Snow and ice-related hazards, risks and disasters (pp. 521-561). (Hazards and disasters series), 2015.

Draebing, D., Krautblatter, M., and Dikau, R.: Interaction of thermal and mechanical processes in steep permafrost rock walls: A conceptual approach, Geomorphology, 226, 226-235, 2014.

Draebing, D., Krautblatter, M., and Hoffmann, T.: Thermo-cryogenic controls of fracture kinematics in permafrost rockwalls, Geophysical Research Letters, 44(8), 3535-3544, 2017.

Draebing, D. and Krautblatter, M.: The Efficacy of Frost Weathering Processes in Alpine Rockwalls, Geophysical Research Letters, 46(12), 6516-6524, 2019.

Duca, S., Occhiena, C., Mattone, M., Sambuelli, L., and Scavia, C.: Feasibility of Ice Segregation Location by Acoustic Emission Detection: A Laboratory Test in Gneiss, Permafrost and Periglacial Processes, 25(3), 208-219, 2014.

Evans, I. S., and Cox, N.: Geomorphometry and the operational definition of cirques, Area, 150-153, 1974.

Ewald, A., Hartmeyer, I., Keuschnig, M., Lang, A., and Otto, J.-C.: Fracture Dynamics In An Unstable, Deglaciating Headwall, Kitzsteinhorn, Austria, EGU General Assembly, Vienna, Austria, 7–12 April 2019, EGU2019-3055, 2019.

Fischer, A.: Calculation of glacier volume from sparse ice-thickness data, applied to Schaufelferner, Austria, Journal of Glaciology, 55, 453-460, 2009.

Fischer, A., Seiser, B., Stocker-Waldhuber, M., Mitterer, C., and Abermann, J.: Tracing glacier changes in Austria from the Little Ice Age to the present using a lidar-based high-resolution glacier inventory in Austria, The Cryosphere, 9, 753-766, 2015.

Gardner, J. S.: Evidence for Headwall Weathering Zones, Boundary Glacier, Canadian Rocky Mountains, Journal of Glaciology, 33(113), 60-67, 1987.

Gilbert, G. K.: Systematic asymmetry of crest lines in the High Sierra of California: Journal of Geology, 12, p. 579–588, 1904.

Gischig, V. S., Moore, J. R., Evans, K. F., Amann, F., and Loew, S.: Thermomechanical forcing of deep rock slope deformation: 1. Conceptual study of a simplified slope, JGR Earth Surface, 116(F4), 2011.

Girard, L., Gruber, S., Weber, S., and Beutel, J.: Environmental controls of frost cracking revealed through in situ acoustic emission measurements in steep bedrock, Geophysical Research Letters, 40(9), 1748-1753, 2013.

Gruber, S., Hoelzle, M., and Haeberli, W.: Rock-wall temperatures in the Alps: modelling their topographic distribution and regional differences, Permafrost and Periglacial Processes, 15(3), 299-307, 2004.

Gruber, S., and Haeberli, W.: Permafrost in steep bedrock slopes and its temperature-related destabilization following climate change, JGR Earth Surface, 112(F2), 2007.

GTN-P: The Global Terrestrial Network for Permafrost, 2020 [Online]. Available: http://gtnp.arcticportal.org/ [Accessed 30.04.2020].

Guglielmin, M., Donatelli, M., Semplice, M., and Capizzano, S.: Ground Surface Temperature Reconstruction for the Last 500 Years Obtained from Permafrost Temperatures Observed in the SHARE STELVIO Borehole, Italian Alps, Climate of the Past, 14, 709–24, 2018.

Haberkorn, A., Phillips, M., Kenner, R., Rhyner, H., Bavay, M., Galos, S. P., and Hoelzle, M.: Thermal regime of rock and its relation to snow cover in steep alpine rock walls: Gemsstock, Central Swiss Alps, Geografiska Annaler Serie A, 97(3), 579-597, 2015.

Haeberli, W. and Hoelzle, M.: Application of inventory data for estimating characteristics of and regional climate-change effects on mountain glaciers: A pilot study with the European Alps, 1995.

Haeberli, W., Hoelzle, M., Paul, F., and Zemp, M.: Integrated monitoring of mountain glaciers as key indicators of global climate change: the European Alps. In: SHARP, M. (ed.) Annals of Glaciology, 46, 2007.

Hall, K.: The role of thermal stress fatigue in the breakdown of rock in cold regions, Geomorphology, 31(1-4), 47-63, 1999.

Hartmeyer, I., Keuschnig, M., and Schrott, L.: A scale-oriented approach for the long-term monitoring of ground thermal conditions in permafrost-affected rock faces, Kitzsteinhorn, Hohe Tauern Range, Austria, Austrian Journal of Earth Sciences, 105(2), 128-139, 2012.

Hartmeyer, I., Delleske, R., Keuschnig, M., Krautblatter, M., Lang, A., Schrott, L., and Otto, J.-C.: Current glacier recession causes significant rockfall increase: The immediate paraglacial response of deglaciating cirque walls, Earth Surface Dynamics Discussion, 2020a.

Hartmeyer, I., Keuschnig, M., Delleske, R., Krautblatter, M., Lang, A., Schrott, L., and Otto, J.-C.: Enhanced rockwall retreat and modified rockfall magnitudes/frequencies in deglaciating cirques from a 6-year LiDAR monitoring, Earth Surface Dynamics Discussion, 2020b.

Hasler, A., Gruber, S., and Beutel, J.: Kinematics of steep bedrock permafrost, JGR Earth Surface, 117(F01016), 2012.

Helfricht, K., Kuhn, M., Keuschnig, M., and Heilig, A.: Lidar snow cover studies on glaciers in the Ötztal Alps (Austria): comparison with snow depths calculated from GPR measurements, The Cryosphere, 8, 41-57, 2014.

Hock, R., G. Rasul, C. Adler, B. Cáceres, S. Gruber, Y. Hirabayashi, M. Jackson, A. Kääb, S. Kang, S. Kutuzov, A. Milner, U. Molau, S. Morin, B. Orlove, and H. Steltzer, 2019: High Mountain Areas. In: IPCC Special Report on the Ocean and Cryosphere in a Changing Climate [H.-O. Pörtner, D.C.

Roberts, V. Masson-Delmotte, P. Zhai, M. Tignor, E. Poloczanska, K. Mintenbeck, A. Alegría, M. Nicolai, A. Okem, J. Petzold, B. Rama, N.M. Weyer (eds.)], 2019.

Holm, K., Bovis, M., and Jakob, M.: The landslide response of alpine basins to post-Little Ice Age glacial thinning and retreat in southwestern British Columbia, Geomorphology, 57(3-4), pp.201-216, 2004.

Hooke, R. L.: Positive feedbacks associated with erosion of glacial cirques and overdeepenings, Geological Society of America Bulletin, 103(8), 1104-1108, 1991.

Jia, H., Xiang, W., and Krautblatter, M.: Quantifying Rock Fatigue and Decreasing Compressive and Tensile Strength after Repeated Freeze-Thaw Cycles, Permafrost and Periglacial Processes, 26(4), 368-377, 2015.

Jia, H., Leith, K., and Krautblatter, M.: Path-Dependent Frost-Wedging Experiments in Fractured, Low-Permeability Granite, Permafrost and Periglacial Processes, 28(4), 698-709, 2017.

Keuschnig, M., Hartmeyer, I., Höfer-Öllinger, G., Schober, A., Krautblatter, M., and Schrott, L.: Permafrost-Related Mass Movements: Implications from a Rock Slide at the Kitzsteinhorn, Austria, in: Engineering Geology for Society and Territory, edited by: Lollino, G., Manconi, A., Clague, J. Shan, W., and Chiarle, M., Springer International Publishing, 1(48), 255-259, 2015.

Keuschnig, M., Krautblatter, M., Hartmeyer, I., Fuss, C., and Schrott, L.: Automated Electrical Resistivity Tomography Testing for Early Warning in Unstable Permafrost Rock Walls Around Alpine Infrastructure, Permafrost and Periglacial Processes, 28(1), 158-171, 2016.

Krautblatter, M., Funk, D., and Günzel, F.: Why permafrost rocks become unstable: a rock-ice-mechanical model in time and space, Earth Surface Processes and Landforms, 38(8), 876-887, 2013.

Lague, D., Brodu, N., and Leroux, J.: Accurate 3D comparison of complex topography with terrestrial laser scanner: Application to the Rangitikei canyon (N-Z), ISPRS Journal of Photogrammetry, 82, 10-26, 2013.

Lambrecht, A. and Kuhn, M.: Glacier changes in the Austrian Alps during the last three decades, derived from the new Austrian glacier inventory. In: SHARP, M. (ed.) Annals of Glaciology, 46, 2007.

Land Salzburg: Waldstandsaufnahme D, Bild 86-88, 24.08.1953, Salzburger Geographisches Informationssystem (SAGIS), Salzburg, Austria, 1953.

Land Salzburg: Laserscanbefligung Bundesland Salzburg 2008, Salzburger Geographisches Informationssystem (SAGIS), Salzburg, Austria, 2008.

Lewis, W. V.: A Melt-water Hypothesis of Cirque Formation, GEOL MAG, 75(6), 249-265, 1938.

Mair, R. and Kuhn, M.: Temperature and movement measurements at a bergschrund, Journal of Glaciology, 40(136), 561-565, 1994.

Matsuoka, N. and Murton, J. B.: Frost weathering: recent advances and future directions, Permafrost and Periglacial Processes, 19(2), 195-210, 2008.

McColl, S. T. and Davies, T. R. H.: Large ice-contact slope movements: glacial buttressing, deformation and erosion, Earth Surface Processes and Landforms, 38(10), 1102-1115, 2012.

Murton, J. B., Kuras, O., Krautblatter, M., Cane, T., Tschofen, D., Uhlemann, S., Schober, S., and Watson, P.: Monitoring rock freezing and thawing by novel geoelectrical and acoustic techniques, JGR Earth Surface, 121(12), 2309-2332, 2016.

Plaesken, R., Keuschnig, M., and Krautblatter M.: Systematic derivation of anchoring forces in permafrost-affected bedrock, EGU General Assembly, Vienna, Austria, 23–28 April 2017, EGU2017-14476, 2017.

Ravanel, L., Magnin, F., and Deline, P.: Impacts of the 2003 and 2015 summer heatwaves on permafrost-affected rock-walls in the Mont Blanc massif, Science of the Total Environment, 609, 132-143, 2017.

Rosser, N. J., Petley, D. N., Lim, M., Dunning, S. A., and Allison, R. J.: Terrestrial laser scanning for monitoring the process of hard rock coastal cliff erosion, Q J ENG GEOL HYDROGE, 38(4), 363-375, 2005.

Sanders, J. W., Cuffey, K. M., Moore, J. R., MacGregor, K. R., and Kavanaugh, J. L.: Periglacial weathering and headwall erosion in cirque glacier bergschrunds, Geology, 40(9), 779-782, 2012.

Sass, O.: Rock Moisture Fluctuations During Freeze-thaw Cycles: Preliminary Results from Electrical Resistivity Measurements, Polar Geography, 28(1), 13-31, 2004.

Scherler, D.: Climatic limits to headwall retreat in the Khumbu Himalaya, eastern Nepal, Geology, 42, 11, 1019-22, 2014.

Schrott, L., Otto, J.-C., and Keller, F.: Modelling alpine permafrost distribution in the Hohe Tauern region, Austria, Austrian Journal of Earth Sciences, 105(2), 169-183, 2012.

Stocker-Waldhuber, M., Fischer, A., Helfricht, K. and Kuhn, M.: Long-term records of glacier surface velocities in the Ötztal Alps (Austria). Earth System Science Data, 11(2), 2019.

Span, N., Kuhn, M., and Schneider, H.: 100 years of ice dynamics of Hintereisferner, Central Alps, Austria, 1894-1994, Annals of Glaciology, 24, 297-302, 1997.

Weber, S., Beutel, J., Faillettaz, J., Hasler, A., Krautblatter, M., and Vieli, A.: Quantifying irreversible movement in steep, fractured bedrock permafrost on Matterhorn (CH), The Cryopshere, 11(1), 567-583, 2017.

Weber, S., Beutel, J., Da Forno, R., Geiger, A., Gruber, S., Gsell, T., Hasler, A., Keller, M., Lim, R., Limpach, P., Meyer, M., Talzi, I., Thiele, L., Tschudin, C., Vieli, A., Vonder Mühll, D., and Yücel, M.: A decade of detailed observations (2008–2018) in steep bedrock permafrost at the Matterhorn Hörnligrat (Zermatt, CH), Earth System Science Data, 11(3), 1203-1237, 2019.

Wegmann, M., Gudmundsson, G., and Haeberli, W.: Permafrost changes in rock walls and the retreat of alpine glaciers: a thermal modelling approach, Permafrost and Periglacial Processes, 9(1), 23-33, 1998.

Weiss, A.: Topographic position and landforms analysis, ESRI user conference, Poster Presentation, San Diego, USA, Vol. 200, 2001.

Zekollari, H., Huss, M., and Farinotti, D.: Modelling the future evolution of glaciers in the European Alps under the EURO-CORDEX RCM ensemble, The Cryosphere, 13(4), 1125-1146, 2019.

Zemp, M., Haeberli, W., Hoelzle, M. & Paul, F.: Alpine glaciers to disappear within decades? Geophysical Research Letters, 33, 2006.